Journal Pre-proofs

Synthesis and evaluation of the HIF-1α inhibitory activity of 3(5)-substituted-4-(quinolin-4-yl)- and 4-(2-phenylpyridin-4-yl)pyrazoles as inhibitors of ALK5

Yan-Wei Li, Xiang-Yu Li, Shanji Li, Li-Min Zhao, Juan Ma, Hu-Ri Piao, Zhe Jiang, Cheng Hua Jin, Xuejun Jin

PII: S0960-894X(19)30791-7
DOI: https://doi.org/10.1016/j.bmcl.2019.126822
Reference: BMCL 126822

To appear in: *Bioorganic & Medicinal Chemistry Letters*

Received Date: 4 September 2019
Revised Date: 3 October 2019
Accepted Date: 10 November 2019

Please cite this article as: Li, Y-W., Li, X-Y., Li, S., Zhao, L-M., Ma, J., Piao, H-R., Jiang, Z., Jin, C.H., Jin, X., Synthesis and evaluation of the HIF-1α inhibitory activity of 3(5)-substituted-4-(quinolin-4-yl)- and 4-(2-phenylpyridin-4-yl)pyrazoles as inhibitors of ALK5, *Bioorganic & Medicinal Chemistry Letters* (2019), doi: https://doi.org/10.1016/j.bmcl.2019.126822

Synthesis and evaluation of the HIF-1α inhibitory activity of 3(5)-substituted-4-(quinolin-4-yl)- and 4-(2-phenylpyridin-4-yl)pyrazoles as inhibitors of ALK5

Yan-Wei Li[a,c,1], Xiang-Yu Li[a,1], Shanji Li[b,1], Li-Min Zhao[a], Juan Ma[a], Hu-Ri Piao[a], Zhe Jiang[c,*], Cheng Hua Jin[a,*], Xuejun Jin[a,*]

[a] *Key Laboratory of Natural Resources of Changbai Mountain and Functional Molecules, Ministry of Education, Molecular Medicine Research Center, College of Pharmacy, Yanbian University, Yanji 133002, PR China.*

[b] *The School of Public Health, Jilin Medical University, Jilin, 132013, PR China.*

[c] *Pharmacy Intravenous Admixture Services, Yanbian University Hospital, Yanji, 133000, PR China*

[*] Corresponding authors.

E-mail addresses: jinchenghua@ybu.edu.cn (C.H. Jin), xjjin@ybu.edu.cn (X. Jin), jiangzhe95@163.com (Z. Jiang).

[1] These authors contributed equally to this work.

Abstract

The transcription factor hypoxia-inducible factor-1α (HIF-1α) plays an important role in apoptosis, metastasis, and proliferation and is recognized as an important potential therapeutic target for cancer. Six series of 3(5)-(6-methylpyridin-2-yl)-4-(quinolin-4-yl)pyrazoles (**11a**–**d**, **12a**–**d**, and **18a**–**d**) and 3(5)-(6-methylpyridin-2-yl)-4-(2-phenyl-pyridin-4-yl)pyrazoles (**19a**–**d**, **20a**–**d**, and **21a**–**d**) were synthesized and evaluated for activin receptor-like kinase 5 (ALK5) and HIF-1α inhibitory activity at the enzyme and cell levels. The effect of the lead compound **20d** (**J-1012**) on HIF-1α activation in HCT116 cells was investigated. **J-1012** markedly decreased the hypoxia-induced or TNF-induced accumulation of HIF-1α protein dose-dependently. Analysis revealed that **J-1012** inhibited HIF-1α protein synthesis, without affecting the degradation of HIF-1α protein. Furthermore, by inhibiting the activation of HIF-1α, **J-1012** suppressed the metastasis and proliferation and promoted apoptosis of HCT116 cells. These results suggest that **J-1012** may be a potential therapeutic agent against human colon cancer.

Keywords: TGF-β; ALK5 inhibitor; HIF-1α; Apoptosis; Docking

Cancer is one of the most serious clinical problems in the world. Statistics from the World Health Organization indicate that cancer accounted for approximately 9.6 million deaths globally in 2018, [1] and the incidence of cancer is increasing every year. As well as surgery and radiation treatment, chemotherapy has been proven to be very useful in cancer therapy.[2,3] Patients treated with conventional cancer chemotherapies usually suffer from side effects of the drugs because of the non-selective action of chemotherapeutic drugs.[4] Thus, the development of potent and effective novel antineoplastic drugs is one of the most intensely persuaded goals of world.

Hypoxia-inducible factor-1 (HIF-1) is composed of α and β subunits. HIF-1α is the most widely expressed isoform, and is regulated mainly post-translationally. In normoxia conditions, the hydroxylation of the HIF-1α protein by prolylhydroxylases causes its degradation by the proteasome,[5] while hydroxylation by the factor inhibiting HIF inhibits HIF-1α binding to CBP/p300.[6] In hypoxia conditions, the proteasomal degradation of HIF-1α is inhibited. Stabilized HIF-1α then dimerizes with HIF-1β and translocates to the nucleus,[7] where it induces the activation of genes containing hypoxia-responsive elements in their promoters.[8] Activated HIF-1 plays an important role in the adaptive responses of tumor cells through the transcriptional activation of over 100 downstream genes that regulate vital biological processes required for tumor survival and progression, including genes involved in cell proliferation and angiogenesis.[9] Although many studies have indicated that HIF-1 is an important regulator of the genetic response to hypoxia, HIF-1α can also be activated by inflammatory cytokines, such as tumor necrosis factor (TNF), interleukin-1β (IL-1β), prostaglandin E2 (PGE2) and lipopolysaccharide (LPS), which suggests that HIF is implicated in the inflammatory process.[10,11] It has recently been shown that certain pro-inflammatory cytokines can stabilize HIF-1α protein expression and activate HIF-1.[12,13] These results suggest that HIF-1 may be involved in the regulation of gene expression during inflammation.

Transforming growth factor-β (TGF-β) is a multifunctional growth factor, which is widely found in the normal tissue cells and transformed cells of animals, and can be produced by almost all cells in the human body.[14] TGF-β family members include

TGF-βs, activins, inhibins, growth and differentiation factors (GDFs), nodal, and anti-Müllerian hormone and bone morphogenetic proteins.[15] TGF-β have three major isoforms such as TGF-β1, TGF-β2, and TGF-β3, which are expressed in mammals, and each isoform is encoded by a unique gene and expressed in a tissue-specific manner. TGF-β is known to regulate cell proliferation, cell migration, extracellular matrix synthesis, and inflammatory processes. Furthermore, TGF-β plays a critical role in the initiation and progression of fibrosis in various organ systems, including the kidneys,[16] heart,[17] lung,[18] and liver.[19] TGF-β transduces signaling through TGF-β type I (activin receptor-like kinase 5, ALK5) and type II receptors.[20] ALK5 is phosphorylated by the combination of TGF-β and the type II receptor, which adjusts its kinase activity.[21] The activated ALK5 phosphorylated Smad2/Smad3 proteins, form a heteromeric complex with Smad4, which is delivered into the nuclei, where it regulate the expression of several hundred genes. Overexpression of TGF-β signaling leaded to various human diseases such as cancer,[22] pancreatic diseases,[23] and hematological malignancies.[24] Hence the regarding TGF-β-mediated ALK5-dependent signaling pathway at the receptor level has been highlighted as a potential method of inhibiting TGF-β signaling. It has been reported that several small molecule ATP-competitive ALK5 inhibitors such as compounds **1** (SB-505124),[25] **2** (SD-208),[26] **3** (A-83-01),[27] **4** (LY-2157299),[28] and **5** (EW-7197),[29] (Fig. 1) inhibited the autophosphorylation of ALK5 and the TGF-β-induced transcription of matrix genes in reporter assays at sub-micromolar concentrations. Compound **2** effectively retarded the progress of fibrosis in the kidney, liver and lung, and compounds **2** and **4** strongly inhibited the growth and invasiveness of cancer cells in animal models. Compound **4** has entered phase II clinical trials against glioma, hepatocellular carcinoma,[30] glioblastoma, and pancreatic cancer.[31–33] In addition, another compound **5**, also entered phase II clinical trials, inhibited TGF-β-induced tumor cell migration and invasion in breast cancer cells, and inhibited hepatic, renal and pulmonary fibrosis by blocking TGF-β/Smad and reactive oxygen species signaling.[34]

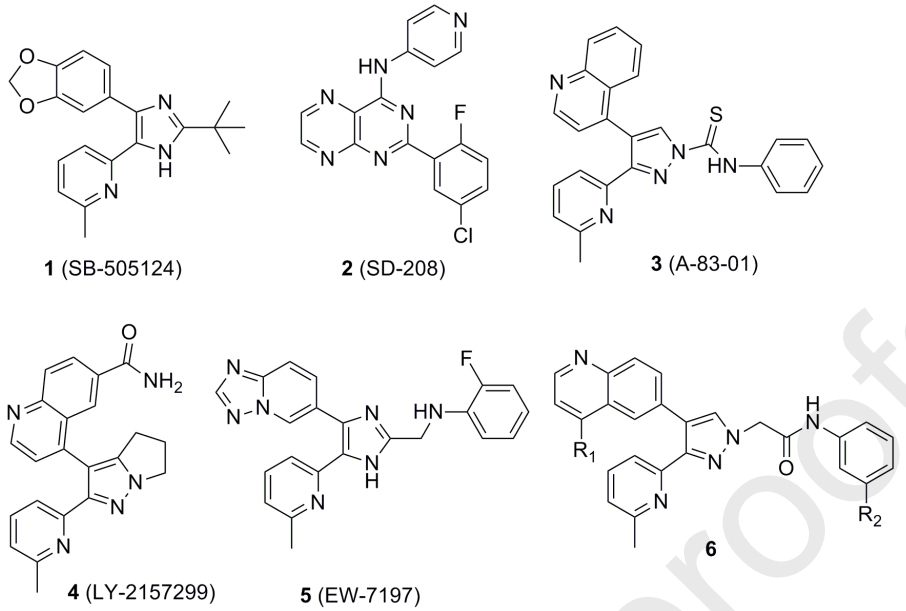

Fig. 1. ALK5 inhibitors under development

A class of ALK5 inhibitors that have a thioamide linkage between a pyrazole ring and a phenyl ring has been reported, and among them, **A-83-01** exhibited significant inhibition of the transcriptional activity induced by ALK5.[27] However, the thioamide linkage was rather unstable and was slowly cleaved, to release the pyrazole ring during long-term storage.

We have previously shown that a series of compounds based on compound **6** containing a quinolin-6-yl moiety, except for the methoxy-substituted analogues, showed significant ALK5 inhibition in an enzymatic assay.[35,36] These compounds showed high selectivity for ALK5 relative to p38α mitogen activated protein (MAP) kinase. Previous studies have shown that ALK5 inhibitors with high selectivity for p38α MAP kinase also show high selectivity for other kinases.[20] The most active compound of the series inhibited ALK5 phosphorylation with an IC_{50} value of 0.022 μM and a selectivity index of >45 against p38α MAP kinase. In this study, we also found that insertion of a methoxy group into the quinoline ring did not improve the ALK5 inhibitory activity of the derivatives, which may be because of steric hindrance from the resulting rigid structures. Therefore, we hypothesized that introducing a methylene group between the pyrazole ring and the thioamide, to give a structure without the rigidity and with less steric hindrance at the 4-positoin of the central

pyrazole ring in compound **3**, may enhance the ALK5 inhibitory activity and the stability. To test this hypothesis, we inserted a methylene group between the pyrazole ring and thioamide, that is, we used a 2-phenylpyridin-4-yl group instead of quinolin-4-yl moiety in compound **3**.

Based on previous research, we replaced the thioamide linkage with a chemically stable thioamidomethylene linkage and, thus, designed compounds **20a–d** and **21a–d** (Fig. 2). To compare the effect of the thioamidomethylene linkage in **20a–d** and **21a–d** on the ALK5 inhibitory activity, the corresponding derivatives **11a–d**, **12a–d**, **18a–d** and **19a–d** with an amidomethylene linkage were also designed. The target compounds **11b–d**, **12b–d**, **18b–d**, **19b–d**, **20b–d**, and **21b–d** each possess a substituent, either *o*-F, *m*-F or *m*-CN on phenyl ring because these substituents were previously found to be beneficial for ALK5 inhibitory activity and selectivity.[29]

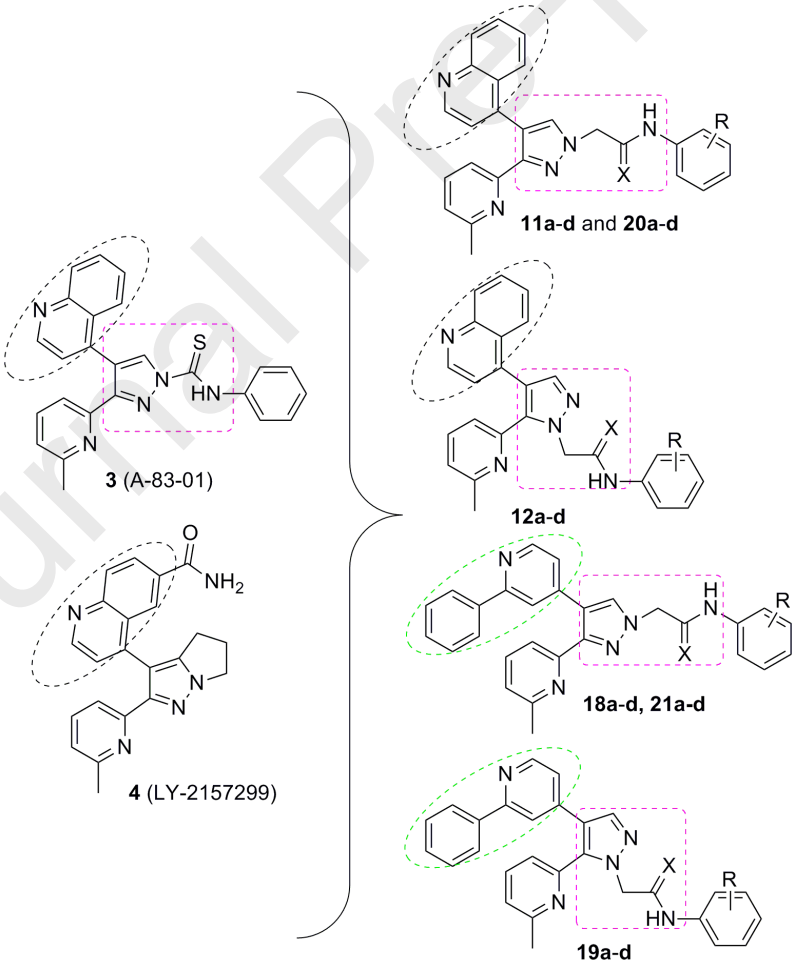

Fig. 2. Design strategy based on compounds **4** and **5**.

In the present study, we explored the antitumor effects of **J-1012** on colon cancer

cells *in vitro*. Based on the combined study results, the following conclusions were reached: (1) **J-1012** suppressed HIF-1 activation. (2) **J-1012** markedly decreased the hypoxia-induced or TNF-induced accumulation of HIF-1α protein dose-dependently. (3) **J-1012** inhibited HIF-1α protein synthesis, without affecting the degradation of HIF-1α protein. (4) **J-1012** by inhibiting the activation of HIF-1α, suppressed metastasis and proliferation and promoted apoptosis. Our findings indicated that **J-1012** could be a valuable preclinical candidate for the development of a cancer therapeutic.

The 3-(6-methylpyridin-2-yl)-4-(quinolin-4-yl)pyrazoles **11a**–**d** was synthesized as shown in Scheme 1. The quinoline-4-carbaldehyde (**7**) was coupled with diphenyl (6-methylpyridin-2-yl)(phenylamino)methylphosphonate[37] in a mixture of THF and *i*-PrOH (4:1) in the presence of Cs_2CO_3 at room temperature, followed by treatment with 1 N HCl to afford the corresponding ketone **8** in 88% yield. Treatment of **8** with *N*,*N*-dimethylformamide dimethyl acetal (DMF•DMA) in DMF at 80°C, followed by cyclization with hydrazine monohydrate in absolute EtOH, produced the pyrazole **9** in 70% yield.[38] The pyrazole **9** was alkylated with substituted phenylacetamides **10a**–**d**[39] in the presence of NaH in anhydrous DMF to yield the target compounds **11a**–**d** and their positional isomer **12a**–**d** in 32%–35% and 7%–15% yields, respectively. The positional isomers were separated by column chromatography and their structures were confirmed by nuclear overhauser enhancement (NOE) experiments. In NOE experiments, irradiation of the methylene protons of compound **11b** at δ 5.17 ppm gave an enhancement of the proton *H*-5 in the pyrazole ring at δ 7.78 ppm, while irradiation of the methylene protons of compound **12b** at δ 5.28 ppm gave no enhancement of the proton *H*-5 in the pyrazole ring at δ 7.86 ppm, confirming the respective alkylation positions.

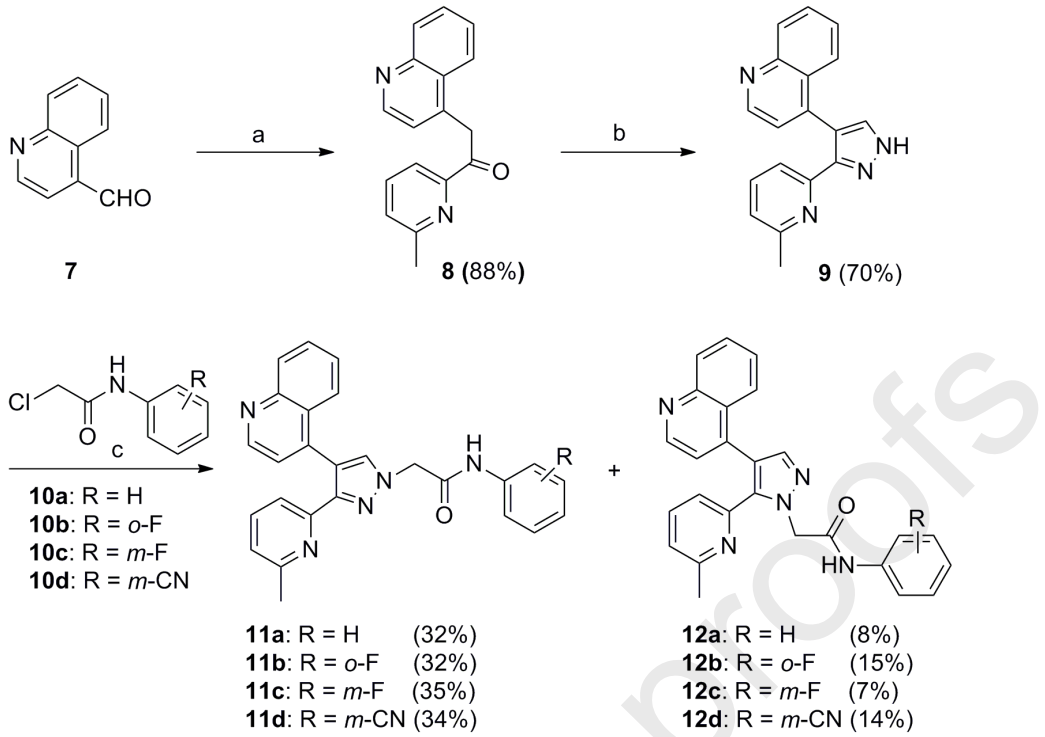

Scheme 1. Reagents and conditions: (a) (i) diphenyl(6-methylpyridin-2-yl)(phenylamino)methylphosphonate, Cs_2CO_3, THF: *i*-PrOH (4:1), rt, 16 h; (ii) 1 N HCl, rt, 1 h; (b) (i) DMF•DMA, DMF, 80°C, 4 h; (ii) N_2H_4•H_2O, EtOH, reflux, 4 h; (c) NaI (cat.), NaH, anhydrous DMF, rt, 2 h.

The 3-(6-methylpyridin-2-yl)-4-(2-phenylpyridin-4-yl)pyrazoles **18a**–**d** was synthesized as shown in Scheme 2. The 2-phenylisonicotinaldehyde (**15**) was synthesized from commercially available phenylboronic acid (**13**) and 2-bromoisonicotinaldehyde (**14**) under Suzuki-Miyaura cross-coupling reaction condition.[40] The target compounds **18a**–**d** and their positional isomers **19a**–**d** were synthesized from compound **15** *via* three steps in the same reaction condition as described in Scheme 1. And these positional isomers were also separated by column chromatography and their structures were confirmed by NOE experiments.

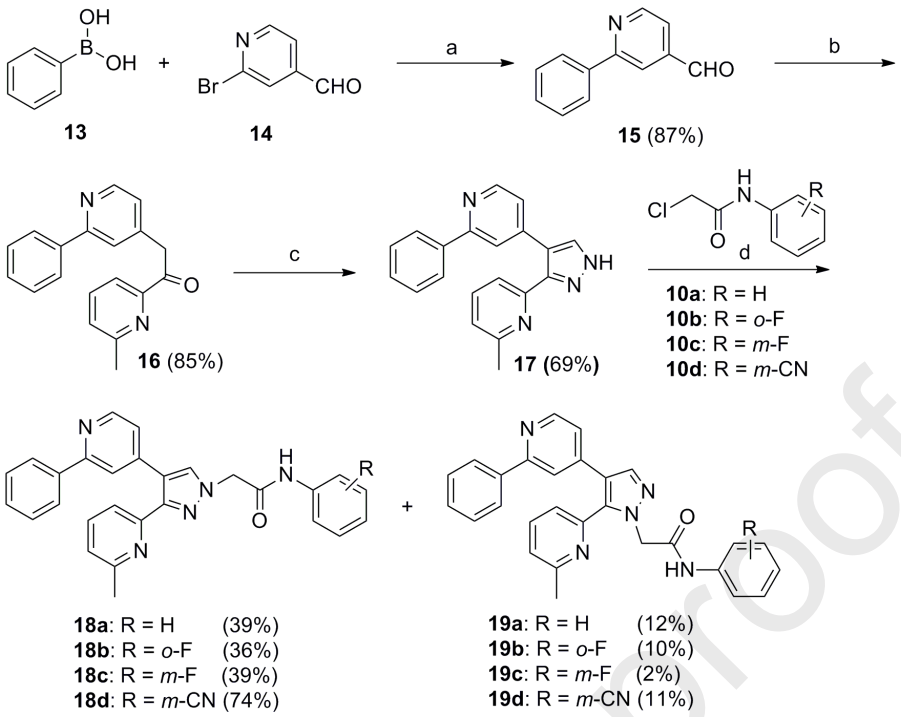

Scheme 2. Reagents and conditions: (a) Na_2CO_3, $Pd(PPh_3)_4$, THF: H_2O (10:1), reflux, 4 h; (b) (i) diphenyl(6-methylpyridin-2-yl)(phenylamino)methylphosphonate, Cs_2CO_3, THF: *i*-PrOH (4:1), rt, 4 h; (ii) 1 N HCl, rt, 1 h; (c) (i) DMF•DMA, DMF, 90°C, 4 h; (ii) $N_2H_4 \cdot H_2O$, EtOH, reflux, 4 h; (d) NaI (cat.), NaH, anhydrous DMF, rt.

Thionation of compounds **11a–d** and **18a–d** with Lawesson´s reagent in anhydrous DME at 85°C produced the thioamides **20a–d** in 33%–97% yields and **21a–d** in 34%–97% yields (Scheme 3). As we expected, all synthesized target compounds were quite stable during long-term storage at room temperature.

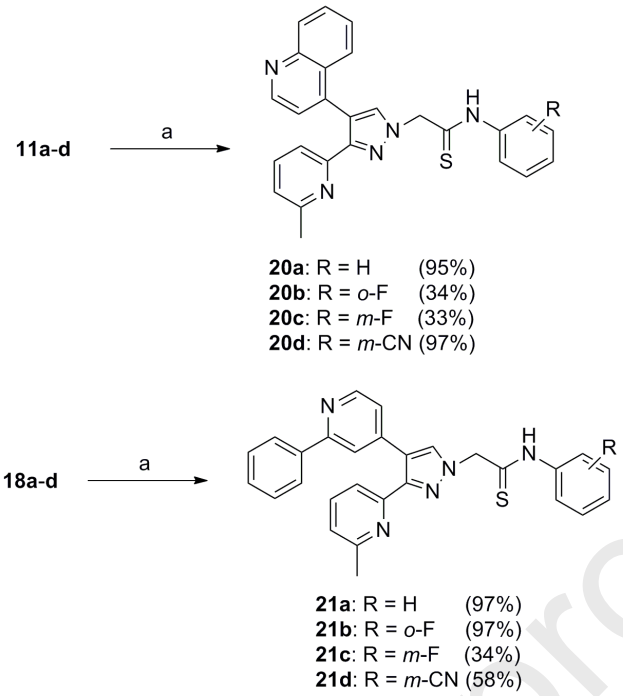

Scheme 3. Reagents and conditions: (a) Lawesson's reagent, 85°C, 4–12 h.

To investigate whether compounds **11a–d**, **12a–d**, **18a–d**, **19a–d**, **20a–d**, and **21a–d** would inhibit ALK5, a kinase assay for preliminary screening was performed using purified human ALK5 kinase domain produced in Sf9 insect cells, and test compounds at 10 μM (Table 1). Compound **4** (LY-2157299) was used as a positive control and DMSO was used as a negative control. All the compounds possessing a quinolin-4-yl moiety (**11a–d**, **12a–d**, and **20a–d**) displayed more potent ALK5 inhibition (21%–100%) than those possessing a 2-phenylpyridin-4-yl moiety (**18a–d**, **19a–d** and **21a–d**, 0%–97%). The amides **11a–d** and **18a–d** showed more potent ALK5 inhibition (98%–100% and 80%–97%, respectively) than their respective positional isomers, **12a–d** (21%–83%) and **19a–d** (0%–7%). Among the compounds containing a quinolin-4-yl moiety, the thioamides **20a–d** showed similar ALK5 inhibition (97%–98%) to their corresponding amides **11a–d** at 10 μM. Among the compounds containing a 2-phenylpyridin-4-yl moiety, the thioamides **21a–d** showed slightly more potent ALK5 inhibition (88%–94%) than the amides **18a–d**, at 10 μM.

We selected p38α MAP kinase to survey the selectivity profile of this series of compounds because its kinase domain is one of the most homologous domains to ALK5.[41] All the tested compounds, except compounds **19a–d** (0%–34% activity), showed good activity (49%–97%) against p38α MAP kinase at 10 μM. Furthermore,

these two series of compounds showed a similar activity pattern to that found for the ALK5 residual assay.

Table 1. Residual activities of 3(5)-(6-methylpyridin-2-yl)-4-(quinolin-4-yl)- and 3(5)-(6-methylpyridin-2-yl)-4-(2-phenylpyridin-4-yl)pyrazoles **11a–d**, **12a–d**, **18a–d**, **19a–d**, **20a–d**, and **21a–d** on ALK5 and p38α MAP kinase

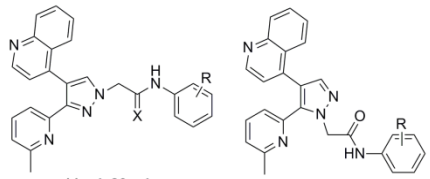

Compound	X	R	Residual activity[a,d]	
			p38α[b]	ALK5[c]
DMSO			100±0.1	100±0.1
11a	O	H	10±0	2±0
11b	O	*o*-F	6±0	0±0
11c	O	*m*-F	4±0	0±0
11d	O	*m*-CN	6±0	1±0
12a	O	H	24±0	71±1.0
12b	O	*o*-F	50±3.5	79±2.5
12c	O	*m*-F	31±0.5	39±4.0
12d	O	*m*-CN	51±3.5	17±1.0
20a	S	H	3±0.5	3±0.5
20b	S	*o*-F	4±0.5	2±0.5
20c	S	*m*-F	3±0.5	2±0.5
20d	S	*m*-CN	3±0	2±0
18a	O	H	11±1.0	12±0.5
18b	O	*o*-F	20±1.5	20±1.0
18c	O	*m*-F	14±0	3±0.5
18d	O	*m*-CN	24±0	18±0
19a	O	H	66±6.0	100±0.5
19b	O	*o*-F	96±3.5	102±2.5
19c	O	*m*-F	81±3.5	93±6.5
19d	O	*m*-CN	135±1.5	105±6.5
21a	S	H	10±1.5	11±1.0
21b	S	*o*-F	4±1.0	11±1.0
21c	S	*m*-F	9±2.5	6±0.5
21d	S	*m*-CN	15±0.5	12±0.5
4 (LY-2157299)			4±0.5	1±0

[a] Residual kinase activities were measured for each compound at 10 μM, in duplicate, in reactions containing p38α and ALK5 protein kinases. [b] p38α MAP kinase was expressed in *E. coli* as the untagged human recombinant protein. [c] ALK5 was expressed in Sf9 insect cells as the human recombinant GST-fusion protein using the vaculovirus expression system. [d] Activity is given as the

mean ± SD of two independent experiments run in duplicate relative to control incubations with DMSO vehicle.

In previous studies, we found that sulfonamide compounds were more active than the corresponding amide compounds.[21,42] To evaluate the ALK5 inhibitory activity and selectivity of the compounds possessing quinolin-4-yl or 2-phenylpyridin-4-yl moieties, the thioamides **20a**–**d** and **21a**–**d** were selected based on residual activity and previous data, and their half maximal inhibitory concentration (IC_{50}) values were measured. All compounds with a quinolin-4-yl moiety (**20a**–**d**) showed potent ALK5 inhibition (IC_{50} = 0.043–0.069 μM), whereas those with a 2-phenylpyridin-4-yl moiety (**21a**–**d**) showed no appreciable ALK5 inhibitory activity (IC_{50} = 1.56–2.20 μM). (Table 2) Compound **20c** showed the most potent ALK5 inhibitory activity of these two series of compounds, with an IC_{50} value of 0.043 μM, which was 2.8-fold more potent than compound **4** (IC_{50} = 0.119 μM). It is noteworthy that these two series of compounds showed good p38α MAPK inhibitory activity (IC_{50} = 0.063–1.15 μM). This result was different to previous data.[21,35] In particular, all compounds with a quinolin-4-yl moiety (**20a**–**d**) showed potent p38α MAPK inhibitory activity (IC_{50} = 0.063–0.104 μM). For all compounds with a 2-phenylpyridin-4-yl moiety (**21a**–**d**), the inhibitory activity towards p38α MAPK was better than towards ALK5. The most potent compound **21b** was 4.2-fold more selective for p38α MAPK (IC_{50} = 0.487 μM) than for ALK5 kinase. (IC_{50} = 2.05 μM). The above result indicated that displacement of the nitrogen atom and insertion of a less rigid structure for the quinolin-4-yl moiety of compound **6** did not appear to improve the selectivity for ALK5 kinase. However, it has been reported that p38α MAPK plays an essential role in cancer and is highly expressed in invasive breast cancers[43] and p38α inhibitors have been shown to be effective for the treatment of p53 mutant and estrogen receptor-negative breast cancers in recent studies.[44] Therefore, these two series of compounds may have potential as anticancer drugs. In these two series of compounds, the effects of the substituents (F and CN) were not obvious.

Table 2. The IC_{50} of 3(5)-(6-methylpyridin-2-yl)-4-(quinolin-4-yl)- and 3(5)-(6-methylpyridin-2-yl)-4-(2-phenylpyridin- 4-yl)pyrazoles **20a**–**d** and **21a**–**d** on ALK5 and p38α MAP kinase

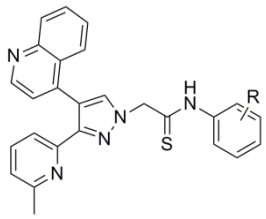

20a-d

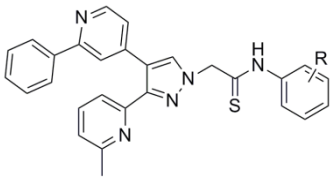

21a-d

Compound	R	IC_{50} (μM)	
		p38α[a]	ALK5[b]
20a	H	0.074±0.0002	0.057±0.0003
20b	*o*-F	0.068±0.0004	0.053±0.0004
20c	*m*-F	0.063±0.0005	0.043±0.0006
20d	*m*-CN	0.104±0.0007	0.069±0.0003
21a	H	0.536±0.0006	1.689±0.0007
21b	*o*-F	0.487±0.0008	2.050±0.0006
21c	*m*-F	0.761±0.0005	1.560±0.0004
21d	*m*-CN	1.150±0.0006	2.200±0.0003
4 (LY-2157299)		0.487±0.0005	0.119±0.0006

[a] p38α MAP kinase was expressed in *E. coli* as untagged human recombinant protein. [b] ALK5 was expressed in Sf9 insect cells as a human recombinant GST-fusion protein using the vaculovirus expression system. [a,b] Values are the average of three independent experiments run in triplicate.

To rationalize the structure-activity relationships (SAR) shown in Tables 1 and 2, we examined the binding modes of two representative ligands, **20b** and **21b**, using the semi-flexible molecular docking programs DS CDOCKER.[45] Docking analyses were performed using the recently reported X-ray structure of ALK5 in complex with a pyrazole ALK5 inhibitor (PDB: 1RWB).[29] As shown in Figure 3, the carbonyl group of Lys337 formed hydrogen bond network with the methylene group, the NH group and the fluoride atom of the side chain of compound **20b**. The quinoline ring in **20b** formed pi-anion interaction and pi-alkyl bond with Lys232. The pyridine ring and pyrazole ring in **20b** formed pi-alkyl bond with Leu340. The phenyl ring of 2-phenylpyridin-4-yl moiety in **21b** formed pi-alkyl bond with Lys232. The pyridine ring of the 2-phenylpyridin-4-yl moiety in **21b** formed pi-alkyl bond with Leu340. The quinolin-4-yl moiety of **20b** and the 2-phenylpyridin-4-yl moiety of **21b** were

stretched to the back of the hydrophobic pocket. Compound **20b** showed higher ALK5 inhibitory activity than compound **21b**, which may be related to the following two reasons. Compound **20b** showed more binding with previously reported key amino acids (Lys337, Glu245, Lys232 and Leu340) than did compound **21b** (Leu340 and Lys232). Not only did the side chain of **21b** not form any bonds with key amino acids, but it was also stretched to the outside of the pocket. Therefore, compound **20b** appeared to be more favorably accommodated in the binding pocket of ALK5 than compound **21b** (Figs. 3B and 3D).

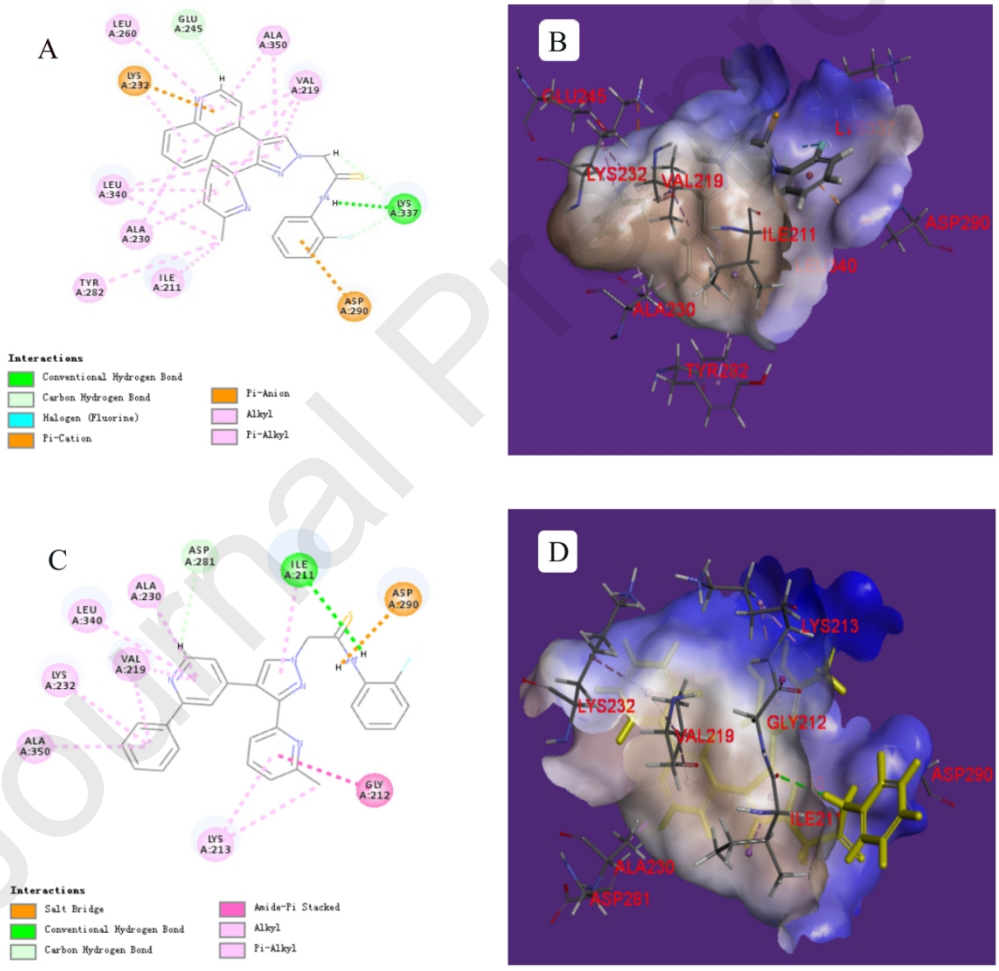

Fig. 3. Docking conformation of compounds **20b** and **21b** in the active site of ALK5 (PDB: 1RWB). (A) 2D binding model of compound **20b**. (B) Proposed conformation of compound **20b** in the binding pocket of ALK5. (C) 2D binding model of compound **21b**. (D). Proposed conformation of compound **21b** in the binding pocket of ALK5. The ligands are shown in yellow.

Both compounds **20b** and **21b** did not form any bonds with Ser280. As bonding

with Ser280 is known to be critical for the selectivity of ligands towards ALK5 over p38α MAP kinase, this may be the reason for the low selectivity of the two compounds. Indeed, the results suggested that the two compounds had a good affinity for p38α related protein. To investigate the binding affinity in the p38α active site, we selected the same compounds (**20b** and **21b**) and examined the binding using DS CDOCKER. The docking performance and accuracy of the DS2017 program was assessed by the semi-flexible docking of the native co-crystalized ligand (SB203580) into p38α MAP-kinase (PDB: 1A9U).[46] As shown in Figure 4, the carboxylic acid group of Asp168 formed a hydrogen bond network with the NH group and the fluoride atom of the side chain of compound **20b**, formed a salt bridge with the NH group of the side chain and a pi-anion bond with the pyrazole ring of compound **20b**. The carboxylic acid group of Glu71 formed a pi-anion bond with the quinoline and pyridine rings of compound **20b**. The two rings of the quinoline in **20b** formed pi-anion bonds with Lys53 and Glu71 and pi-alkyl bonds with Ala51 and Ile84. The pyridine ring in compound **20b** formed a pi-anion bond with Lys53 and a pi-cation bond with Glu71. The carboxylic acid group of Glu71 formed a pi-cation bond with the phenyl ring of the 2-phenylpyridin-4-yl moiety of compound **21b**. The pyridine ring of the 2-phenylpyridin-4-yl moiety in compound **21b** formed a pi-alkyl bond with Lys53. The carboxylic acid of Asp168 formed a hydrogen bond with the NH group of the side chain of compound **21b** and a pi-cation bond with the pyrazole ring. Compound **20b** showed higher p38α inhibitory activity than compound **21b**, which may be related to the following two reasons. Compound **20b** showed more bonding with previously reported key amino acids (Asp168, Ala51, Lys53, Ile84, and Glu71) than did compound **21b** (Asp168, Lys53, and Glu71).[46,47] Moreover, compound **21b** was more stretched out to the edge of the p38α binding pocket than compound **20b** (Figs. 4C and 4D). Hence, compound **20b** appeared to be more favorably accommodated in the binding pocket of p38α than compound **21b**.

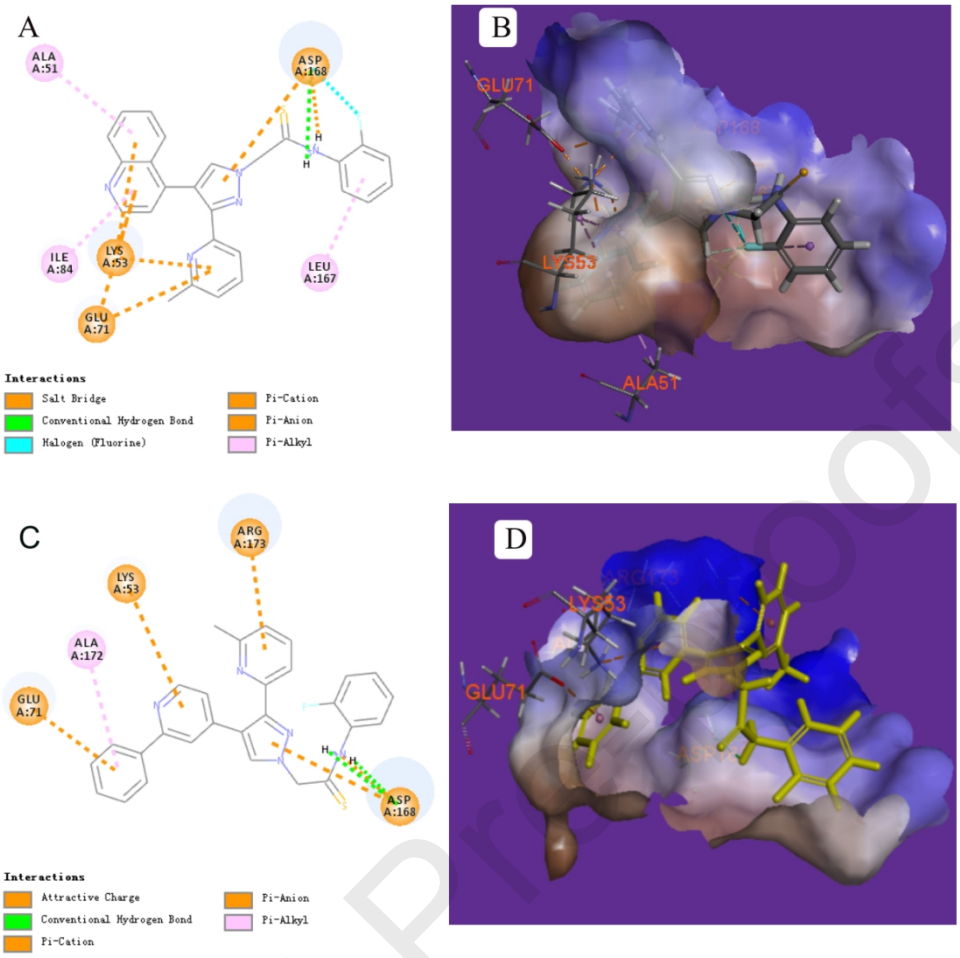

Fig. 4. Docking conformation of compounds **20b** and **21b** in the active site of p38α (PDB: 1A9U). (A) 2D binding model of compound **20b**. (B) Proposed conformation of compound **20b** in the binding pocket of p38α. (C) 2D binding model of compound **21b**. (D). Proposed conformation of compound **21b** in the binding pocket of p38α. The ligands are shown in yellow.

The HIF-1α inhibitory activity of all compounds (**20a–d** and **21a–d**) was evaluated and the pretest results showed that compound **20d** (**J-1012**) had the best activity. To explore the interaction between **J-1012** and HIF-1α, the binding mode was investigated through a molecular docking study. It was shown that the pyridine moiety and side chain of **J-1012** were stretched into the back of the binding pocket consisting of Arg342, Thr301, Cys308, Phe263, His307, Ser262, and Gln320. The nitrogen atom on the side chain of Gln320 formed hydrogen bonds with the pyridine and central pyrazole ring of **J-1012**. The carboxylic acid group of Phe263 formed a

hydrogen bond with the NH group of the side chain of **J-1012** (Figs. 5A and 5B). Subsequently, to investigate the effect of **J-1012** on the transcriptional activity of HIF-1, we transfected HCT116 cells with a luciferase reporter gene driven by six specific HREs. A significant increase in luciferase activity was observed in cells cultured under hypoxic conditions, while **J-1012** dose-dependently inhibited hypoxia-induced luciferase activity (Fig. 5C). To evaluate the effect of **J-1012** on cell viability in HCT116 cells, a MTT assay was performed. **J-1012** did not display significant cellular toxicity towards HCT116 cells at concentrations up to 50 μM (Fig. 5D).

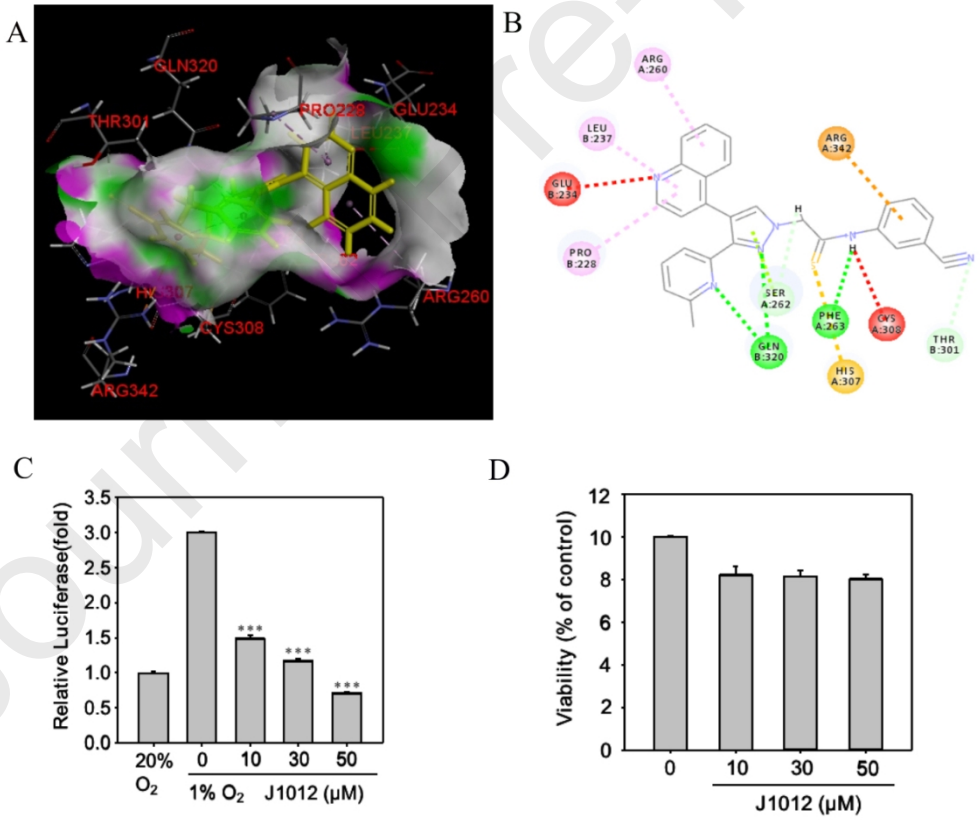

Fig. 5. A) **J-1012** was docked into the binding site of HIF-1α (3D binding mode). The ligand is shown yellow. B) **J-1012** was docked into the binding site of HIF-1α (2D binding mode). C) HCT116 cells were transiently co-transfected with a pGL3-HRE-Luciferase and pRL-CMV vectors. Following 24 h incubation, the cells were incubated under hypoxia in the absence or presence indicated concentrations

of **J-1012**. Luciferase activities were determined as described in "Materials and Methods". Data represented as mean ± standard deviation of three independent experiments. $^{**}p < 0.01$, $^{***}p < 0.001$, significant with respect to control. D) MTT assay to measure cell viability in HCT116 cell after 24 h treatment with the indicated concentrations of **J-1012** concentrations.

To explore the effects of **J-1012** on HIF-1α expression under hypoxic conditions, HIF-1α protein levels were determined in HCT116 cells treated with **J-1012**. Following 12 h treatment, **J-1012** exhibited dose-dependent inhibition of the HIF-1α protein levels induced by hypoxia in HCT116 cells (Fig. 6A). Several studies have demonstrated that some inflammatory cytokines, such as TNF, IL-1β, and LPS, can induce the transcriptional activity of HIF-1α.[48] Thus, we exposed HCT116 cells to the inflammatory factor TNF (10 ng/mL) for 12h. TNF dramatically promoted HIF-1α protein expression and **J-1012** inhibited this TNF-induced HIF-1α protein expression (Fig. 6B); **LY-2157299**, the positive control group, had a similar effect to that of **J-1012**. Generally, the accumulation of HIF-1α protein is dependent on the balance between HIF-1α protein synthesis and degradation.[49] To further investigate whether the mechanism of inhibition was the result of increased degradation, or decreased synthesis, of HIF-1α protein, the proteasome inhibitor MG-132 was used to prevent HIF-1α protein degradation. After treatment with MG-132, the level of HIF-1α protein was significantly increased under hypoxic conditions (lane 2 compared with lane 4 in Fig. 6C). In contrast, **J-1012** inhibited HIF-1α accumulation even under co-treatment with MG-132 (lanes 3 and 5 in Fig. 6C). These results indicated that HIF-1α protein synthesis in HCT116 cells is markedly impaired in the presence of **J-1012**. Next, to investigate the effect of **J-1012** on the stability of the HIF-1α protein, the protein translation inhibitor CHX was used to prevent HIF-1α protein synthesis. We first induced HIF-1α accumulation by exposing the cells to 1% O_2 for 4 h, and then added CHX alone or in conjunction with **J-1012**. Under these conditions, the HIF-1α protein levels reflected the rate of HIF-1α degradation. In the presence of CHX, the HIF-1α levels declined rapidly as expected, however, **J-1012** did not alter the degradation rate of HIF-1α (Fig. 6D).

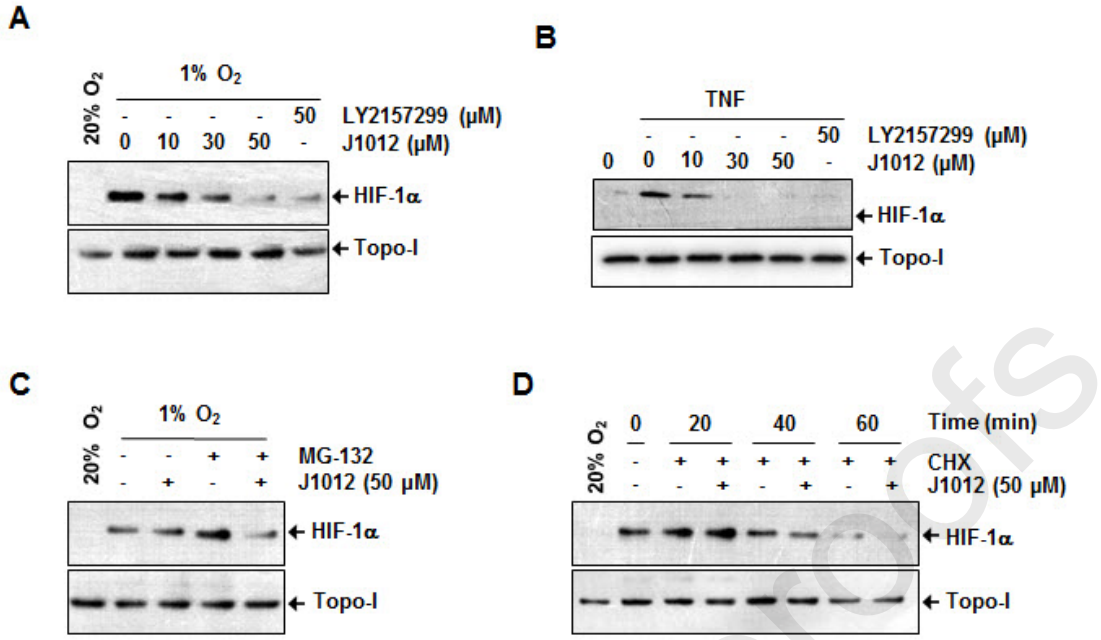

Fig. 6. A) HCT116 cell were incubated under normoxia, or hypoxia conditions for 12h, in the indicated concentration of **J-1012**, or **LY-2157299** (50 μM). Nuclear extracts were then prepared and assayed for HIF-1α protein expressions by western blotting. The same blot was reprobed with an anti-Topo-I antibody as a loading control. B) HCT116 cell were exposed to 10 ng/mL TNF for 24 h and incubated concentration of **J-1012**, or **LY-2157299** (50 μM). Total protein of the HCT116 cells was extracted, and the HIF-1α expression levels were then detected by western blotting. The same blot was reprobed with an anti-Topo-I antibody as a loading control. C) HCT116 cells were pretreatment with proteasome inhibitor MG-132 (10 μM) for 30 min and incubated with **J-1012** (50 μM) in the presence of 1% O_2. After 12 h incubation, the nuclear extract for HIF-1α was analyzed by Western blotting. The same blot was reprobed with an anti-Topo-I antibody as a loading control. D) Mix cycloheximide (CHX) (10 μM) and **J-1012** (50 μM) with medium and treated HCT116 cells. After 20, 40, 60 min incubation, the nuclear extract for HIF-1α was analyzed by Western blotting. The same blot was reprobed with an anti-Topo-I antibody as a loading control.

Recent studies have strongly suggested that HIF-1α acts as a potent inducer of cell apoptosis.[50] We wondered if **J-1012** could enhance the apoptosis induced by TNF. To test our hypothesis, we carried out Annexin V-FITC/PI double staining. As shown in Figs 7A and 7B, treatment of HCT116 cells with vehicle only, TNF alone, **J-1012** alone, **LY-2157299** alone, TNF and **LY-2157299** combined treatment, and TNF and **J-1012** combined treatment induced apoptosis by 1.2%, 4%, 6.3%, 5.3%, 6.5% and 8%, respectively. Because caspases are a group of cysteine proteases critical for the apoptosis of eukaryotic cells, we investigated whether **J-1012** affected the TNF-induced activation of caspase-8 and caspase-3. TNF alone had only a minimal effect, and **J-1012** alone significantly affected the activation of caspase-8 and

caspase-3, whereas co-treatment with TNF and **J-1012** potentiated activation of the caspases, as indicated by the presence of cleaved caspases (Fig. 7C, top three panels). In addition, the PARP cleavage assay was used to detect TNF-induced apoptosis. **J-1012** potentiated the effect of TNF-induced PARP cleavage, although **J-1012** alone also induced PARP cleavage (Fig. 7C, bottom second panel). These results indicate that **J-1012** (50 μM) could significantly enhance the TNF-induced apoptosis of HCT116 cells compared with **LY-2157299** (50 μM) (Fig. 7A).

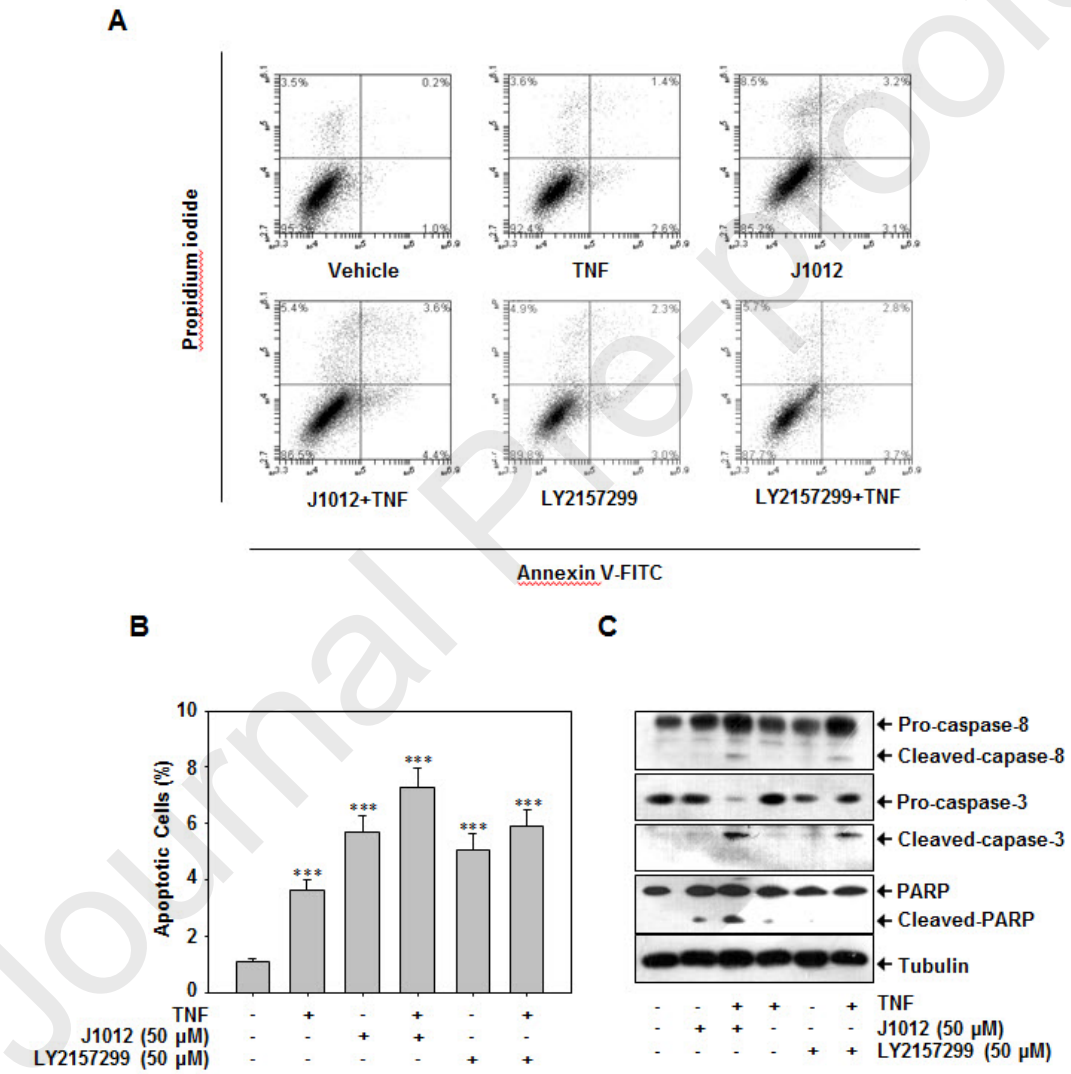

Fig. 7. A) HCT116 cells were pretreated with 50 μM **J-1012** or 50 μM **LY-2157299** for 12 h and then incubated with TNF (10 ng/mL) for 24 h, and stained with Annexin V-FITC and propidium iodide (PI), followed by analysis using a flow cytometer. Early apoptotic cells (Annexin-V^+ and PI^-) are displayed in the lower right quadrant and late apoptotic cells (Annexin-V^+ and PI^+) are shown in the upper right quadrant. B) The percentage of apoptotic cells was counted. C) HCT116 cells were pretreated with 50 μM **J-1012** or 50 μM **LY-2157299** for 12 h and then incubated with TNF (10 ng/mL) for 24 h, Whole cell extracts were analyzed by western blot analysis using indicated antibodies for cleaved caspase-8,

cleaved capase-3, cleaved PARP and tubulin.

Previous studies have demonstrated that the HIF-1α regulated expressions of VEGF, MMP-9 and ICAM-1 is involved in tumor-cell proliferation, angiogenesis, invasion and metastasis.[51,52] We therefore examined whether **J-1012** can suppress the expression of these proteins. VEGF, MMP-9 and ICAM-1 protein levels were measured by western blot analysis in HCT116 cells. The results indicated that TNF induced the expression of ICAM-1, MMP-9 and VEGF, whereas **J-1012** inhibited the expression (Fig. 8A). These results were also reflected in the mRNA levels (Fig. 8B). The migration of endothelial cells is a prerequisite for solid tumor angiogenesis.[53] The cell scratch assay was performed to examine the influence on the motile activity of HUVECs. The results showed that **J-1012** (50 μM) could significantly inhibit the TNF-induced migration and invasive capacity of HCT116 cells compare with **LY-2157299** (50 μM).

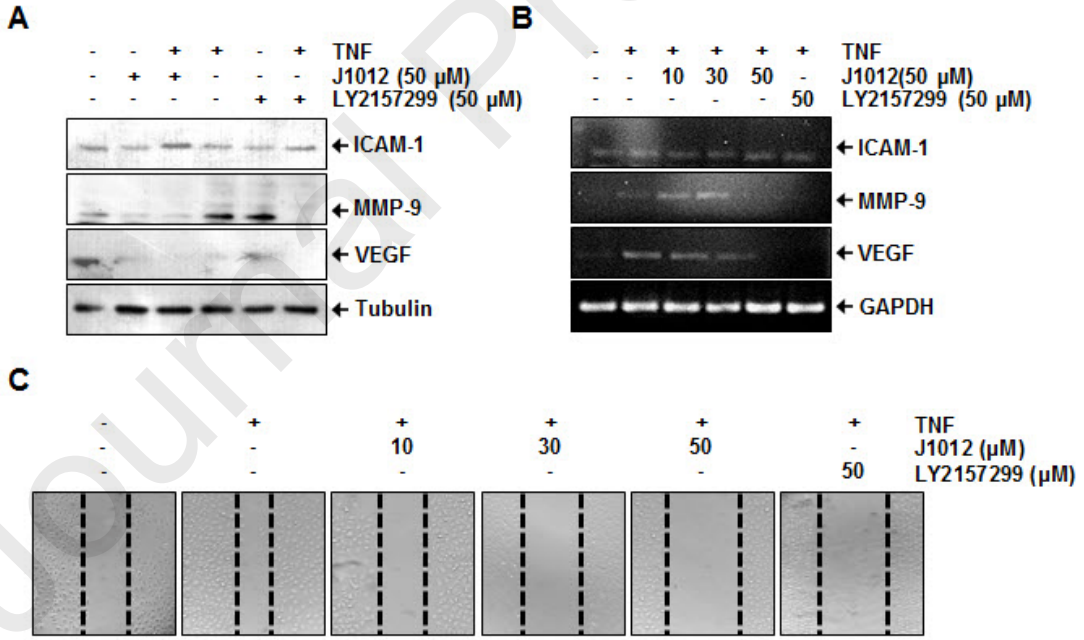

Fig. 8. A) HCT116 cells were pretreated with 50 μM **J-1012** or 50 μM **LY-2157299** for 12 h and then incubated with TNF (10 ng/mL) for 24 h, Whole cell extracts were analyzed by western blot analysis using indicated antibodies for ICAM-1, MMP-9, VEGF and tubulin. B) HCT116 cells were preincubated with indicated concentrations of **J-1012** or 50 μM **LY-2157299** for 12 h, and then treated with 10 ng/mL TNF for an additional 12 h. The expression levels of ICAM-1, VEGF, MMP-9 were verified by RT-PCR. GAPDH was used to show equal loading of total RNA. C) HUVEC cells were pretreatment with indicated concentrations of **J-1012** or 50 μM **LY-2157299** in the presence or absence

of TNF (10 ng/mL). Photographs at time after 24 h are shown. The area delimited with dashed line represents the uncovered area.

To determine whether **J-1012** could affect cell proliferation, the Edu incorporation assay was performed. Following 12 h treatment, **J-1012** (50 μM) inhibited the number of Edu-positive cells induced by TNF in HCT116 cells. **J-1012** (50 μM) significantly inhibited the proliferation of HCT116 cells compared with **LY-2157299** (50 μM) (Figs. 9A and 9C). To determine the effect of the long-term antiproliferative activity of **J-1012**, we used a colony formation assay. The results showed that the levels of HCT116 cells were reduced in a dose-dependent manner (Figs. 9B and 9D) by **J-1012**.

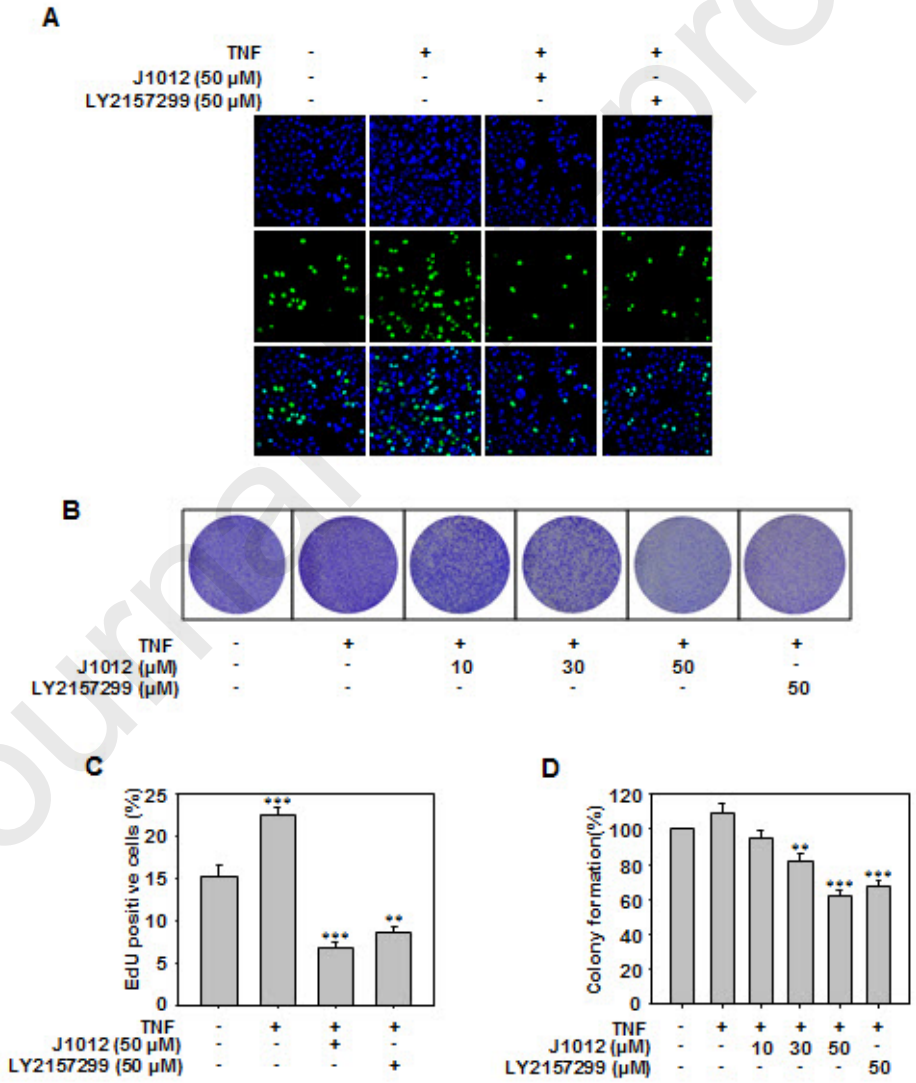

Fig. 9. A) HCT116 cells were incubated with **J-1012** (50 μM) or **LY-2157299** (50 μM) for 12 h and treated with TNF (10 ng/ml) for 30 min. The EdU-labeled proliferations cells were examined under a fluorescence microscope. B) HCT116 cells treated with **J-1012** 10, 30 50 μM or 50 μM **LY-2157299**

for 12 h and then treated with TNF (10 ng/ml) for 30 min. Next, the medium was replaced with a new one. Keep cell growing for 10 days. Finally, the cells were stained with crystal violet and photographed. C), D) Data represented as mean ± standard deviation of three independent experiments. *$p < .05$, **$p < .01$, ***$p < .001$.

HIF-1 is overexpressed in many human cancers, and the activity of HIF-1 in cells is correlated with tumorigenicity and angiogenesis.[54] Under normal oxygen tension, HIF-1α binds to the von Hippel-Lindau protein and is degraded *via* the ubiquitin-dependent pathway.[55] During this process, specific proline residues undergo posttranslational hydroxylation by prolyl hydroxylases.[56] In hypoxic conditions, HIF-1 is stabilized and complexes with the β subunit to form a functional transcription factor. The complete HIF-1 molecule translocates to the nucleus and activates the expression of downstream genes in response to hypoxia.[57] In this way, HIF-1 activates different genes involved in angiogenesis, migration and survival, such as erythropoietin and VEGFs.[52,58] The same genes are often found to be overexpressed in tumor cells, suggesting that these pathways are also involved in tumor progression, development, invasion, metastasis, apoptosis and tumorigenesis.[49,52,59] Therefore, HIF-1 plays an important role in tumorigenesis and development. Inhibition of HIF-1 activity has been shown to have a considerable effect on tumor growth in preclinical studies.[60,61] The development of HIF-1 inhibitors represents a major challenge in the field of cancer treatment. In this study, we demonstrated that **J-1012** inhibited HIF-1α levels by impairing HIF-1α protein synthesis.

With the expression of HIF-1α, tumor cells express high levels of VEGF and interact with the VEGF receptor 2 (VEGFR2) to induce the growth of vascular endothelial cells, the proliferation of endothelial cells and the formation of new vessels.[62] Cadherin and inter-cellular adhesion molecule-1 (ICAM-1) are adhesion molecules that affect the adhesion, invasion and metastasis of tumor cells.[62] In the present study, we have shown that **J-1012** suppressed TNF-induced MMP-9, ICAM-1 and VEGF mRNA levels.

Apoptosis plays an important role in the regulation of tumor cell growth, metastasis, and invasion. Our study demonstrated that **J-1012** potentiated TNF-induced apoptosis

of HCT116 cells, which was confirmed from flow cytometry analysis. Apoptosis is characterized by specific morphological and biochemical features in which caspase activation plays a central role. In this study, we found that **J-1012** affected the TNF-induced activation of caspase-8 and caspase-3, and PARP cleavage, indicating that the apoptotic effects of TNF are enhanced by cryptopleurine. **J-1012** also inhibited TNF-induced HIF-1α protein expression.

In this report, six series of 3(5)-(6-methylpyridin-2-yl)-4-(quinolin-4-yl)pyrazoles (**11a**–**d**, **12a**–**d** and **18a**–**d**) and 3(5)-(6-methylpyridin-2-yl)-4-(2-phenyl-pyridin-4-yl)- pyrazoles (**19a**–**d**, **20a**–**d** and **21a**–**d**) were synthesized and evaluated for ALK5 inhibitory activity in enzymatic assays. We found that the introduction of a quinolin-4-yl moiety at the 4-position of the pyrazole ring improved the inhibitory activity towards ALK5, while the introduction of a 2-phenylpyridin-4-yl moiety at the same position did not improve the inhibitory activity. The most potent compound, **20c**, inhibited ALK5 phosphorylation with an IC_{50} value of 0.043 μM, and exhibited 98% inhibition of ALK5 phosphorylation, at a concentration of 10 μM in an enzymatic assay. Molecular docking studies were performed to identify the mechanism of action of the test compounds and good binding interactions were observed. The results of the docking studies supported the conclusion that the ring size of the heterocycle at the 4-position in 1-substituted-3-(6-methylpyridin-2-yl)pyrazoles may be important for good ALK5 inhibition. Furthermore, the present study showed that **J-1012** can inhibit HIF-1α activity in HCT116 cells. In addition, we elucidated an important mechanism of the anticancer activity of **J-1012**, related to cell invasion, metastasis, proliferation and apoptosis, which are essential factors for tumor progression. This mechanism may in part explain the anticancer effect of **J-1012**, and provides a rationale for the development of **J-1012** as an anticancer drug. Further studies need to be performed in colon cancer patients to determine the clinical utility of **J-1012**.

Acknowledgments

This work was partially supported by the National Science Foundation of China (No. 81560557, 81760657 and 81660608) and the Education Department of Jilin Province Scientific Research Fund Project (No. 2016-283). This work was partially supported by Jilin Province Science and Technology Development Outstanding Young Talents (20180520057JH) and Yanbian University Youth Research Fund Project (2017.No. 31) and the 13th five-year program of science and technology of the ministry of education of jilin province (JJKH20191152KJ). We thank Victoria Muir, PhD, from Liwen Bianji, Edanz Group China (www.liwenbianji.cn/ac), edited the English text of a draft of this manuscript.

Supplementary data

Supplementary data associated with this article can be found, in the online version.

References

1. Wu J, Zhang ZH, Zhang LH, et al. *Bioorg Med Chem Lett.* 2019;29:853.
2. Reddy CN, Nayak VL, Mani GS, et al. *Bioorg Med Chem Lett.* 2015;25:4580.
3. Kamel MM, Megally Abdo NY. *Eur. J. Med. Chem*. 2014;86:75.
4. Muhamad N, Plengsuriyakarn T, Na-Bangchang K. *Int J Nanomedicine*. 2018;13:3921.
5. Maxwell PH, Dachs GU, Gleadle JM, et al. *Proc Natl Acad Sci USA*. 1997;94:8104.
6. Lando D, Peet DJ, Gorman JJ, et al. *Genes Dev*. 2002;16:1466.
7. Jiang BH, Zheng JZ, Leung SW, et al. *J. Biol. Chem*. 1997;272:19253.
8. Gray MJ, Zhang J, Ellis LM, et al. *Oncogene.* 2005;24:3110.
9. Masoud GN, Li W. *Acta. Pharm. Sin B*. 2015;5:378.
10. Blouin CC, Pagé EL, Soucy GM, et al. *Blood*. 2004;103:1124.
11. Haddad JJ, Land SC. *FEBS Lett*. 2001;505:269.
12. Patten DA, Lafleur VN, Robitaille GA, et al. *Mol Biol Cell*. 2010;21:3247.
13. Pagé EL, Robitaille GA, Pouysségur J, et al. *J Biol Chem*. 2002;277:48403.
14. Serita S, Tomokiyo A, Hasegawa D, et al. *Arch Oral Biol*. 2017;78:135.
15. Schmierer B, Hill CS. *Nature Rev Mol Cell Biol*. 2007;8:970.
16. Jeong BY, Park SR, Cho S, et al. *J Antimicrob Chemoth*. 2018;73:962.
17. Lim H, Zhu YZ. *Cell Mol Life Sci*. 2006;63:2584.
18. Gu L, Zhu YJ, Yang X, et al. *Acta Pharmacol Sin*. 2007;28:382.
19. Zhang D, Hao X, Xu L, et al. *Oncol Lett*. 2017; 14:4511.
20. Zhao LM, Guo Z, Xue YJ, et al. *Molecules*. 2018;23:3369/1.
21. Jin CH, Sreenu D, Krishnaiah M, et al. *Eur J Med Chem*. 2011;46:3917.
22. Hendrik U, Frank G, Roland K, et al. *Int J Mol Sci*. 2018;19:1568/1.
23. Tobias B, Benjamin R, Dirk R, et al. *Mol Cancer*. 2015;14:199/1.
24. Dong M, Blobe GC. *Blood*. 2006;107:4589.
25. Byfield SD, Major C, Laping NJ, et al. *Mol Pharmacol*. 2004;65:744.
26. Uhl M, Aulwurm S, Wischhusen J, et al. *Cancer Res*. 2004;64:7954.
27. Tojo M, Hamashima Y, Hanyu A, et al. *Cancer Sci*. 2005;96:791.
28. Bueno L, De Alwis DP, Pitou C, et al. *Eur J Cancer*. 2008;44:142.
29. Jin CH, Krishnaiah M, Sreenu D, et al. *J Med Chem*. 2014;57:4213.
30. Giannelli G, Villa E, Lahn M. *Cancer Res*. 2014;74:1890.
31. Mundla SR. *World Patent WO 2007018818 A1*. 2007.
32. Fujiwara Y, Nokihara H, Yamada Y, et al. *Cancer Chemother Pharmacol*. 2015;76:1143.
33. Brandes AA, Carpentier AF, Kesari S, et al. *Neuro-Oncology*. 2016;18:1146.
34. Park SA, Kim MJ, Park SY, et al. *Cell Mol Life Sci*. 2015;72:2023.
35. Jin CH, Krishnaiah M, Sreenu D, et al. *Bioorg Med Chem*. 2011;19:2633.

36. Zhu WJ, Cui BW, Wang HM, et al. *Eur J Med Chem*. 2019;180:15.

37. Journet M, Cai D, Larsen RD, et al. *Tetrahedron Lett*. 1998;39:1717.

38. Sun LH, Niu DQ, Lee WC, et al. *World Patent WO 2009009059 A1*. 2009.

39. Mridula S, Agarwal SK, Patnaik GK, et al. *J Med Chem*. 1990;33:2970.

40. Hamed A, Christoph B, Christine B, et al. *World Patent WO 2012063207 A1*. 2012.

41. Eyers PA, Craxton M, Morrice N, et al. *Chem Biol*. 1998;5:321.

42. Zhao LM, Guo Z, Xue YJ, et al. Molecules. 2018;23:3369/1.

43. Chen L, Mayer JA, Krisko TI, et al. *Cancer Res*. 2009;69:8853.

44. Dyrager C, MÖllers LN, Kjäll LK, et al. *J Med Chem*. 2011;54:7427.

45. Wang ZC, Qin YJ, Wang PF, et al. *Eur J Med Chem*. 2013;66:1.

46. Lopes RDO, Romeiro NC, Lima CDFD, et al. *Eur J Med Chem*. 2012;54:264.

47. Gill K, Singh AK, Kapoor V, et al. *Biochim Biophys Acta*. 2013;1830:2763.

48. Tang M, Tian Y, Li D, et al. *PLoS One*. 2014;9:102967/1.

49. Wang JY, Wang Z, Li M, et al. *Chem Biol Interact*. 2018;296:134.

50. Greijer AE, van der Wall E. *J Clin Pathol*. 2004;57:1009.

51. Zhou B, Zhan H, Tin L, et al. *Cancer Lett*. 2016;382:11.

52. Semenza GL. Nat Rev Cancer. 2003;3:721.

53. Zheng LC, Wang XQ, Lu K, et al. *Oncotarget*. 2017;8:41348.

54. Wilson WR, Hay MP. *Nat Rev Cancer*. 2011;11:393.

55. Dai Y, Bae K, Siemann DW. *Int J Radiat Oncol Biol Phys*. 2011;81:521.

56. Loboda A, Jozkowicz A, Dulak J. *Mol Cells*. 2010;29:435.

57. Wang G, Wang JJ, Fu XL, et al. *Oncol Rep*. 2017;37:657.

58. Semenza GL. *J Clin Invest*. 2013;123:3664.

59. Semenza GL, Roth PH, Fang HM, et al. *J Biol Chem*. 1994;269:23757.

60. Vaupel P. *Oncologist*. 2004;9:10.

61. Wouters A, Pauwels B, Lardon, F, et al. *Oncologist*. 2007;12:690.

62. Petersen LH, Dzialowski E, Huggett DB. *Comp Biochem Physiol A Mol Integr Physiol*. 2011;160:311.

Figure captions:

Table 1. Residual activities of compounds **11a**–**d**, **12a**–**d**, **18a**–**d**, **19a**–**d**, **20a**–**d**, and **21a**–**d** on ALK5 and p38α MAP kinase

Table 2. The IC_{50} of compounds **20a**–**d** and **21a**–**d** on ALK5 and p38α MAP kinase

Fig. 1. ALK5 inhibitors under development

Fig. 2. Design strategy based on compounds **4** and **5**

Fig. 3. Docking of compounds **20b** and **21b** in the active site of ALK5

Fig. 4. Docking of compounds **20b** and **21b** in the active site of p38α

Fig. 5. Identification of **J-1012** as a HIF-1 pathway inhibitor from a cell-based screening assay

Fig. 6. Effect of **J-1012** on HIF-1α protein synthesis

Fig. 7. Effect of **J-1012** on the TNF-induced apoptosis in HCT116 cells

Fig. 8. Effect of **J-1012** on the TNF-induced invasion

Fig. 9. **J-1012** inhibits the proliferation of cells.

Scheme 1. Synthetic scheme for the synthesis of compounds **11a**–**d** and **12a**–**d**

Scheme 2. Synthetic scheme for the synthesis of compounds **18a**–**d** and **19a**–**d**

Scheme 3. Synthetic scheme for the synthesis of compounds **20a**–**d** and **21a**–**d**

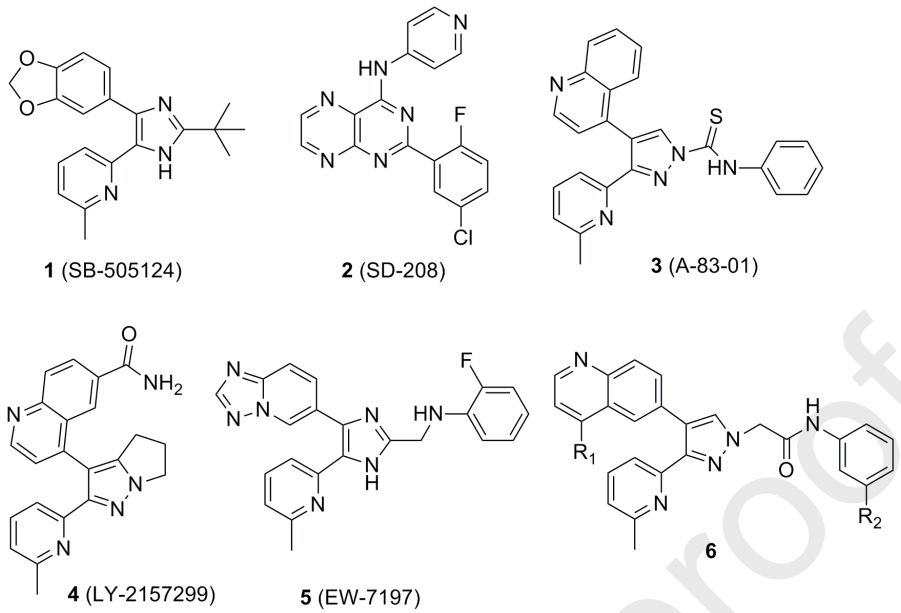

Fig. 1. ALK5 inhibitors under development

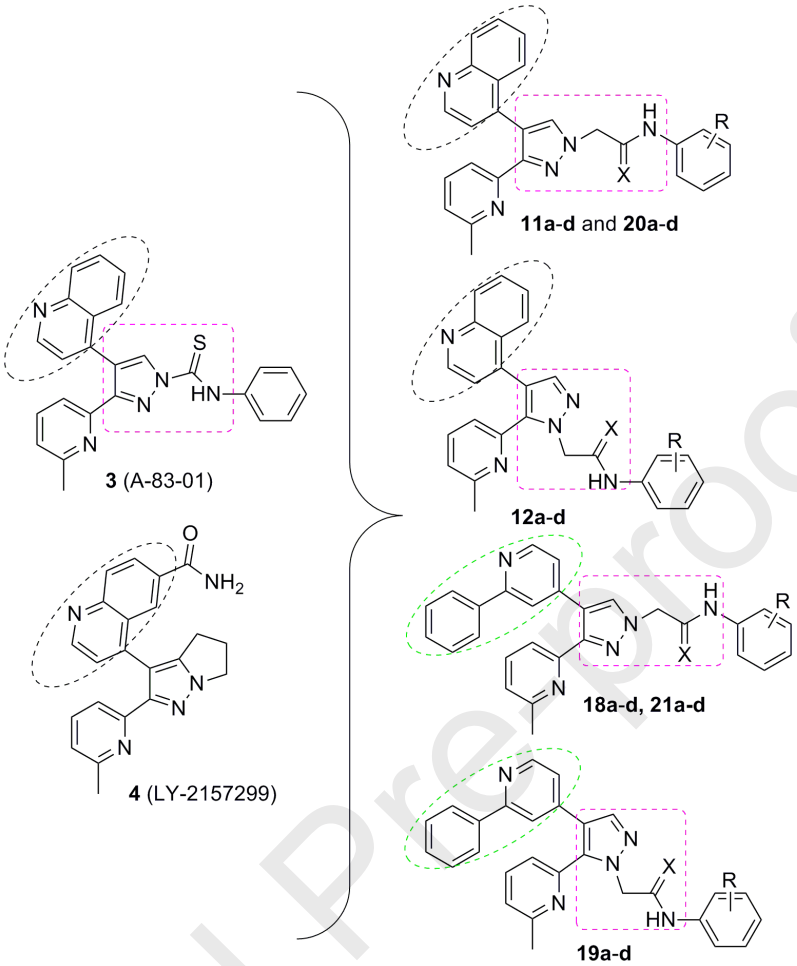

Fig. 2. Design strategy based on compounds **4** and **5**.

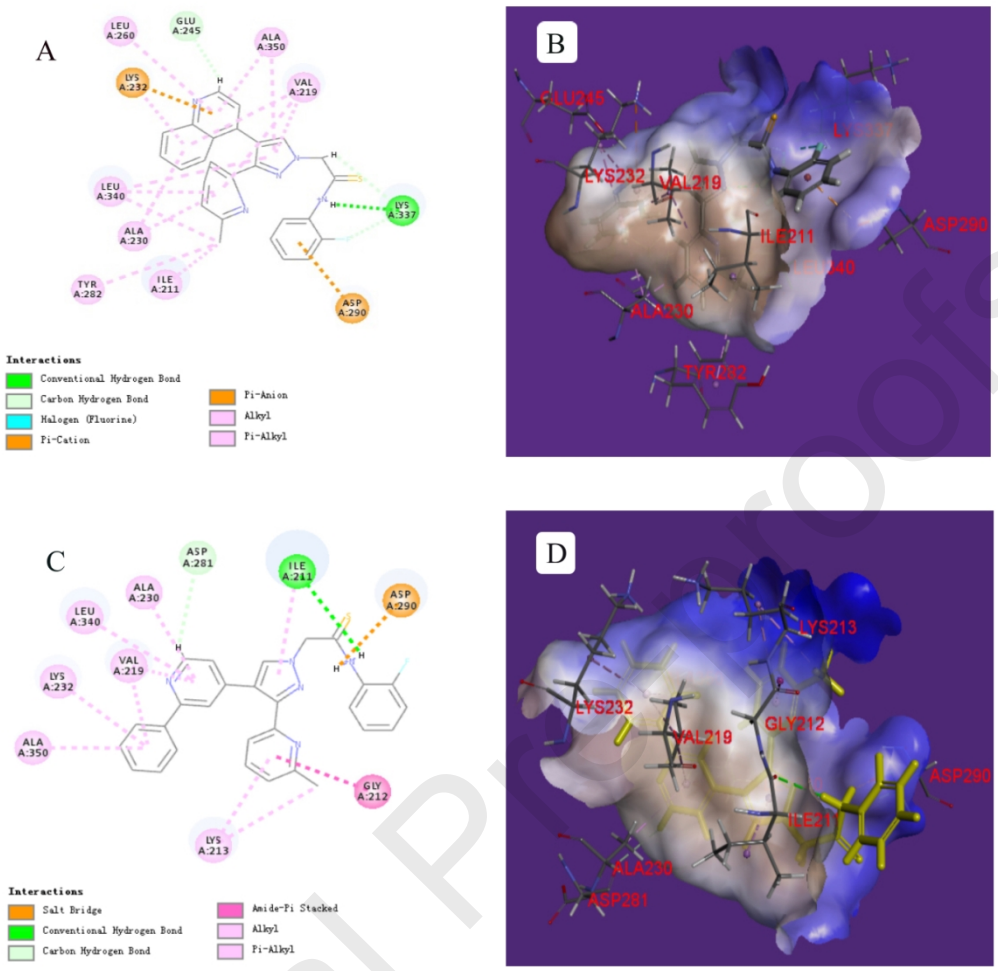

Fig. 3. Docking conformation of compounds **20b** and **21b** in the active site of ALK5 (PDB: 1RWB). (A) 2D binding model of compound **20b**. (B) Proposed conformation of compound **20b** in the binding pocket of ALK5. (C) 2D binding model of compound **21b**. (D). Proposed conformation of compound **21b** in the binding pocket of ALK5. The ligands are shown in yellow.

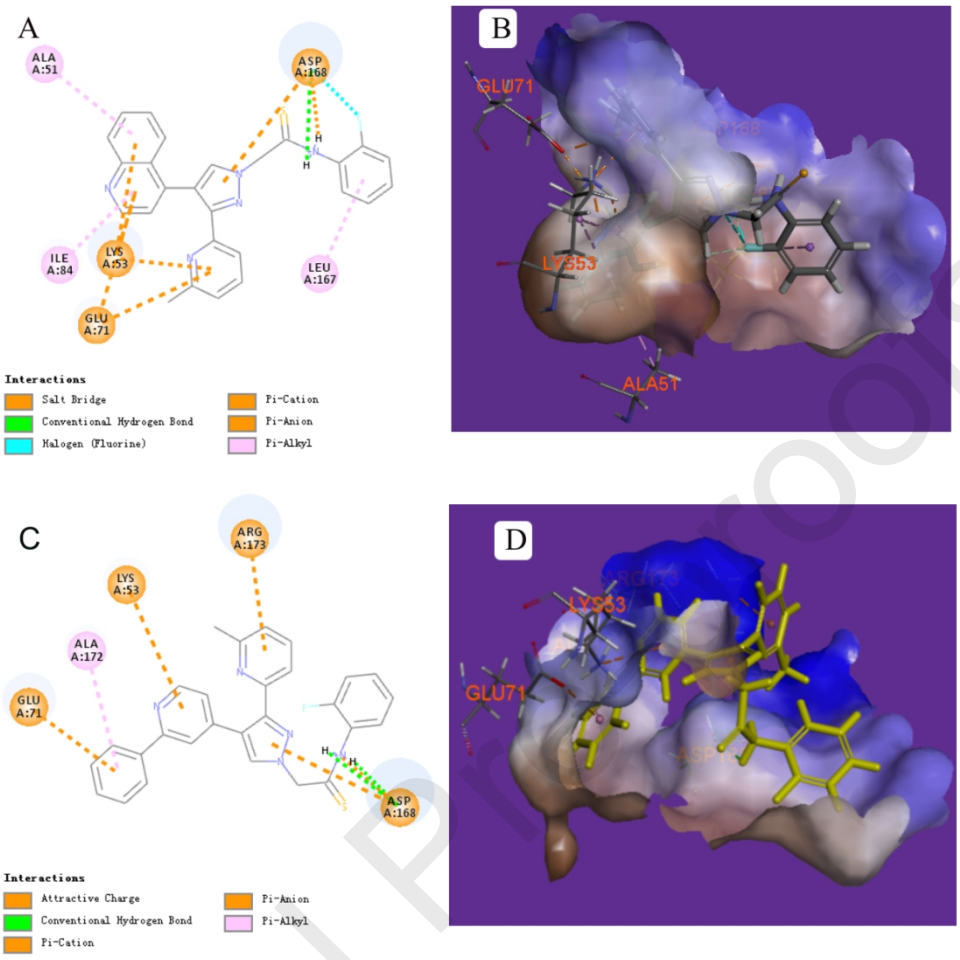

Fig. 4. Docking conformation of compounds **20b** and **21b** in the active site of p38α (PDB: 1A9U). (A) 2D binding model of compound **20b**. (B) Proposed conformation of compound **20b** in the binding pocket of p38α. (C) 2D binding model of compound **21b**. (D). Proposed conformation of compound **21b** in the binding pocket of p38α. The ligands are shown in yellow.

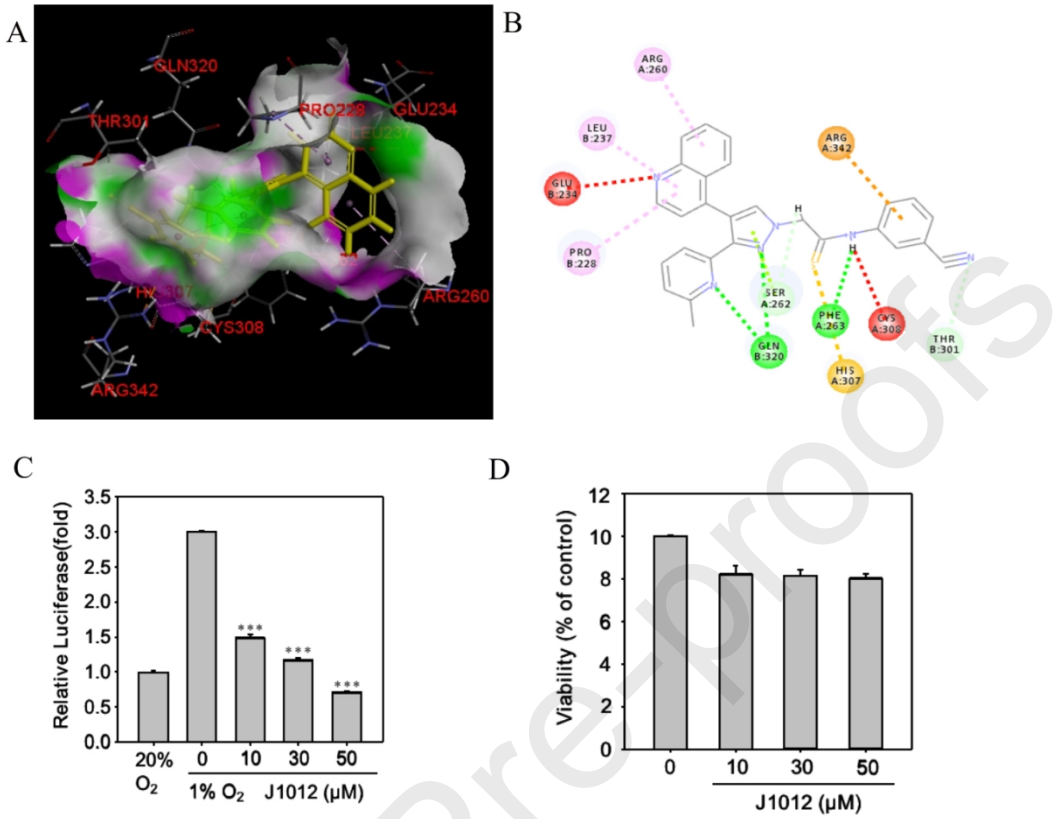

Fig. 5. A) **J-1012** was docked into the binding site of HIF-1α (3D binding mode). The ligand is shown yellow. B) **J-1012** was docked into the binding site of HIF-1α (2D binding mode). C) HCT116 cells were transiently co-transfected with a pGL3-HRE-Luciferase and pRL-CMV vectors. Following 24 h incubation, the cells were incubated under hypoxia in the absence or presence indicated concentrations of **J-1012**. Luciferase activities were determined as described in "Materials and Methods". Data represented as mean ± standard deviation of three independent experiments. $^{**}p < 0.01$, $^{***}p < 0.001$, significant with respect to control. D) MTT assay to measure cell viability in HCT116 cell after 24 h treatment with the indicated concentrations of **J-1012** concentrations.

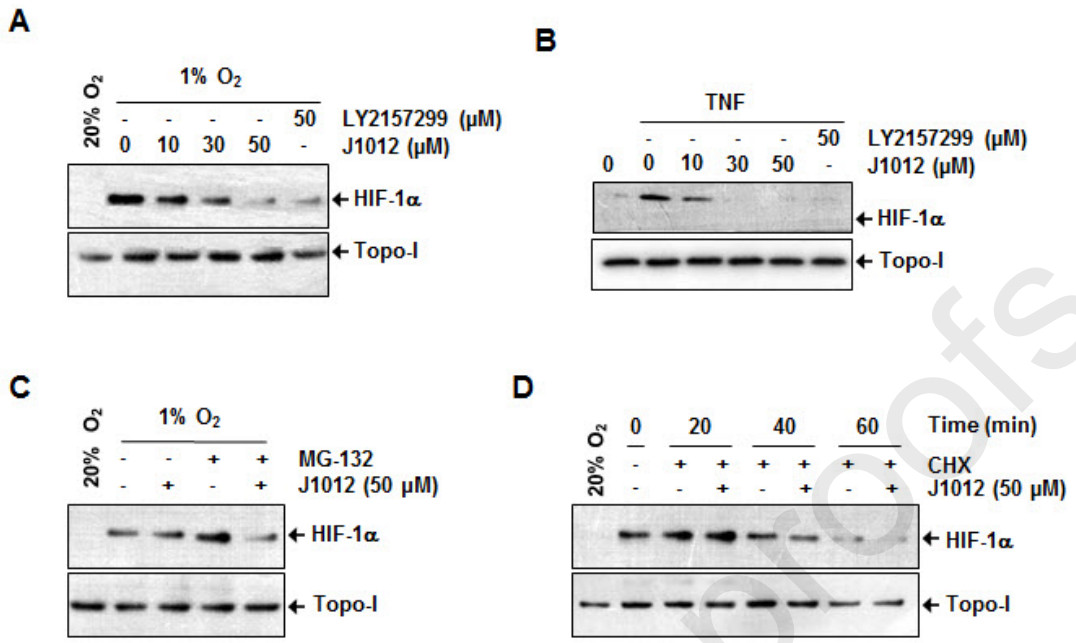

Fig. 6. A) HCT116 cell were incubated under normoxia, or hypoxia conditions for 12h, in the indicated concentration of **J-1012**, or **LY-2157299** (50 μM). Nuclear extracts were then prepared and assayed for HIF-1α protein expressions by western blotting. The same blot was reprobed with an anti-Topo-I antibody as a loading control. B) HCT116 cell were exposed to 10 ng/mL TNF for 24 h and incubated concentration of **J-1012**, or **LY-2157299** (50 μM). Total protein of the HCT116 cells was extracted, and the HIF-1α expression levels were then detected by western blotting. The same blot was reprobed with an anti-Topo-I antibody as a loading control. C) HCT116 cells were pretreatment with proteasome inhibitor MG-132 (10 μM) for 30 min and incubated with **J-1012** (50 μM) in the presence of 1% O_2. After 12 h incubation, the nuclear extract for HIF-1α was analyzed by Western blotting. The same blot was reprobed with an anti-Topo-I antibody as a loading control. D) Mix cycloheximide (CHX) (10 μM) and **J-1012** (50 μM) with medium and treated HCT116 cells. After 20, 40, 60 min incubation, the nuclear extract for HIF-1α was analyzed by Western blotting. The same blot was reprobed with an anti-Topo-I antibody as a loading control.

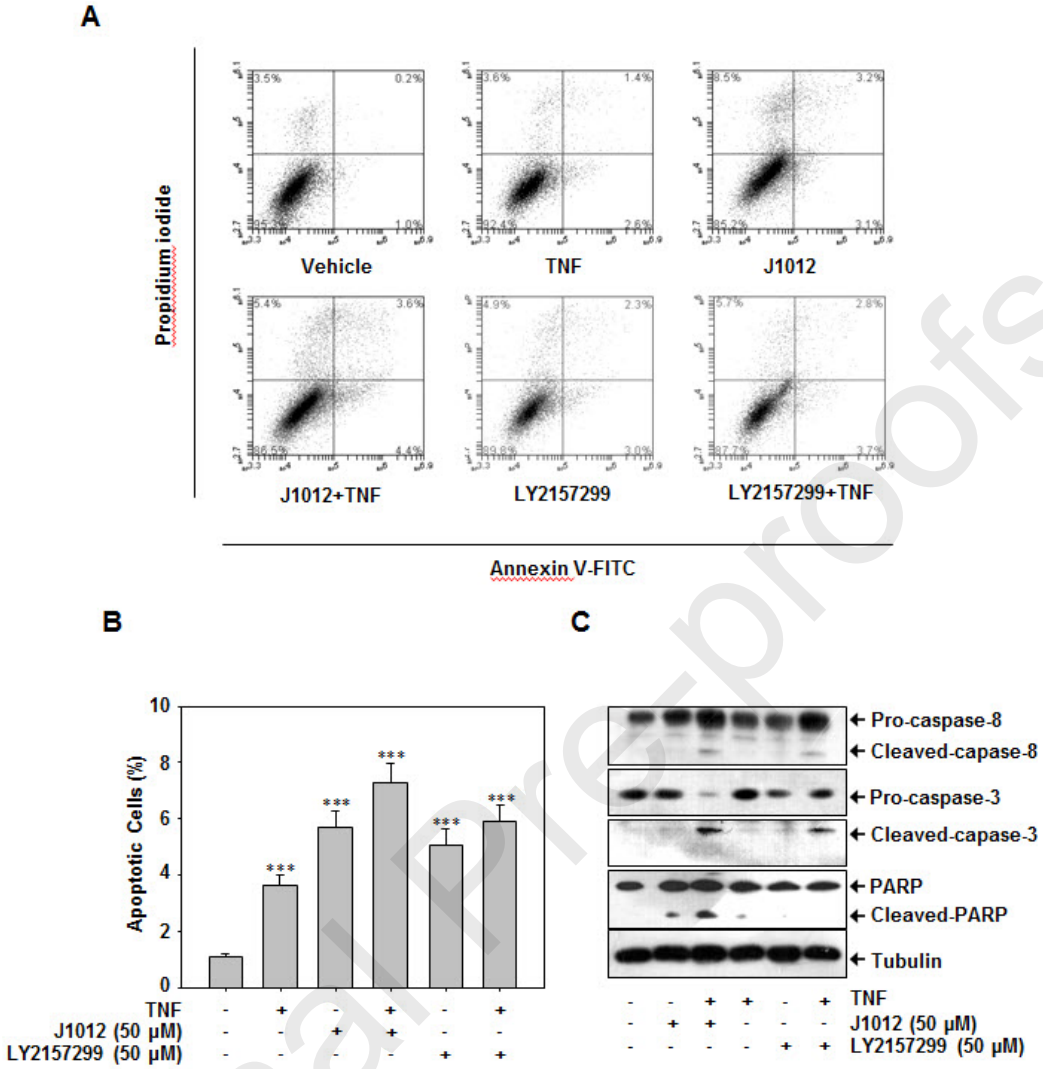

Fig. 7. A) HCT116 cells were pretreated with 50 μM **J-1012** or 50 μM **LY-2157299** for 12 h and then incubated with TNF (10 ng/mL) for 24 h, and stained with Annexin V-FITC and propidium iodide (PI), followed by analysis using a flow cytometer. Early apoptotic cells (Annexin-V^+ and PI^-) are displayed in the lower right quadrant and late apoptotic cells (Annexin-V^+ and PI^+) are shown in the upper right quadrant. B) The percentage of apoptotic cells was counted. C) HCT116 cells were pretreated with 50 μM **J-1012** or 50 μM **LY-2157299** for 12 h and then incubated with TNF (10 ng/mL) for 24 h, Whole cell extracts were analyzed by western blot analysis using indicated antibodies for cleaved caspase-8, cleaved capase-3, cleaved PARP and tubulin.

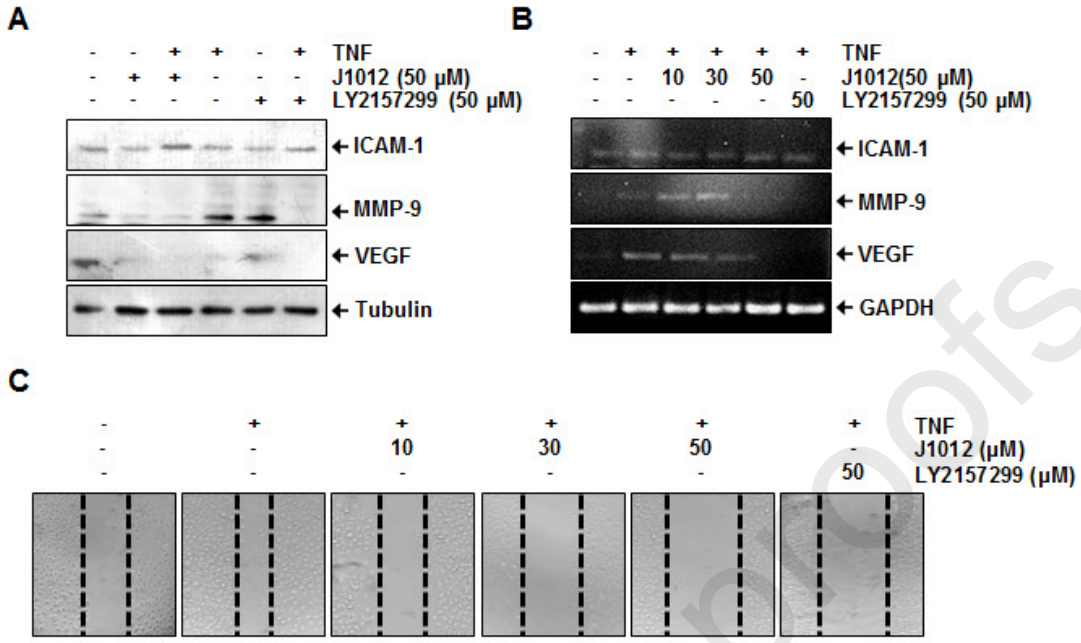

Fig. 8. A) HCT116 cells were pretreated with 50 μM **J-1012** or 50 μM **LY-2157299** for 12 h and then incubated with TNF (10 ng/mL) for 24 h, Whole cell extracts were analyzed by western blot analysis using indicated antibodies for ICAM-1, MMP-9, VEGF and tubulin. B) HCT116 cells were preincubated with indicated concentrations of **J-1012** or 50 μM **LY-2157299** for 12 h, and then treated with 10 ng/mL TNF for an additional 12 h. The expression levels of ICAM-1, VEGF, MMP-9 were verified by RT-PCR. GAPDH was used to show equal loading of total RNA. C) HUVEC cells were pretreatment with indicated concentrations of **J-1012** or 50 μM **LY-2157299** in the presence or absence of TNF (10 ng/mL). Photographs at time after 24 h are shown. The area delimited with dashed line represents the uncovered area.

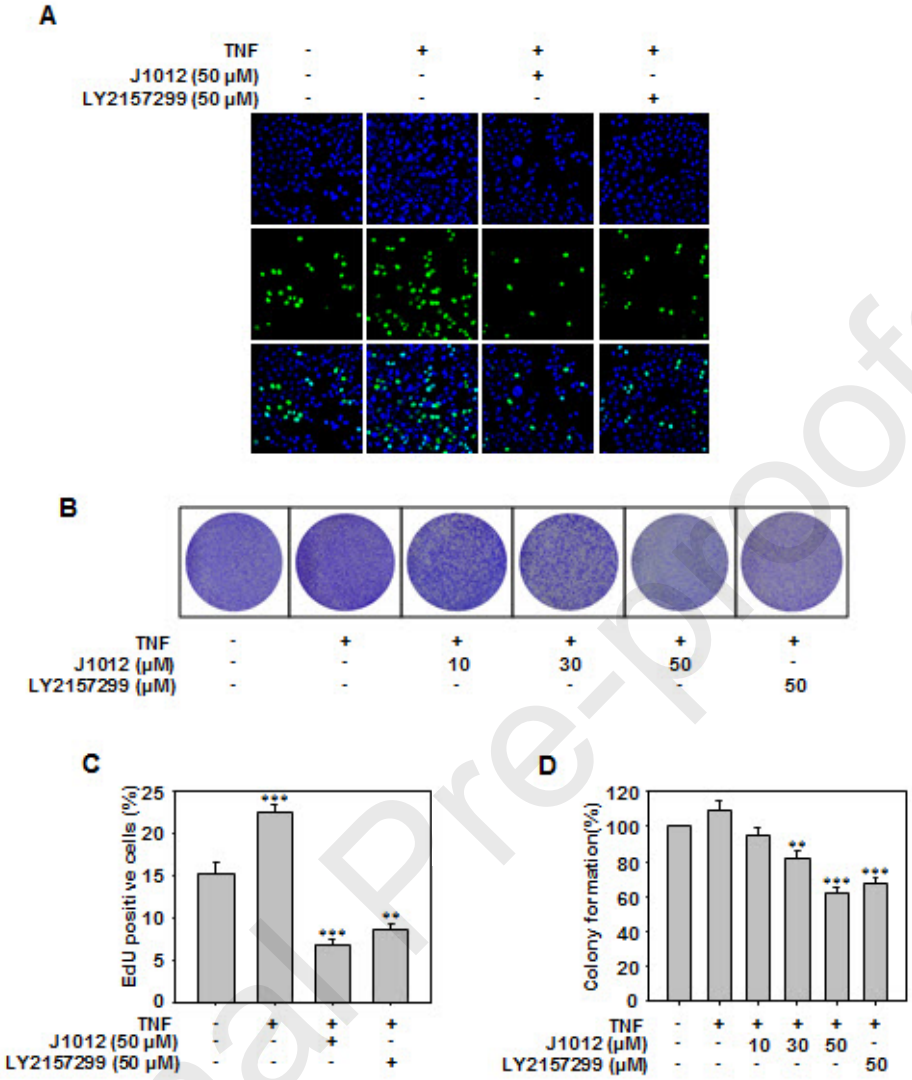

Fig. 9. A) HCT116 cells were incubated with **J-1012** (50 μM) or **LY-2157299** (50 μM) for 12 h and treated with TNF (10 ng/ml) for 30 min. The EdU-labeled proliferations cells were examined under a fluorescence microscope. B) HCT116 cells treated with **J-1012** 10, 30 50 μM or 50 μM **LY-2157299** for 12 h and then treated with TNF (10 ng/ml) for 30 min. Next, the medium was replaced with a new one. Keep cell growing for 10 days. Finally, the cells were stained with crystal violet and photographed. C), D) Data represented as mean ± standard deviation of three independent experiments. *$p < .05$, **$p < .01$, ***$p < .001$.

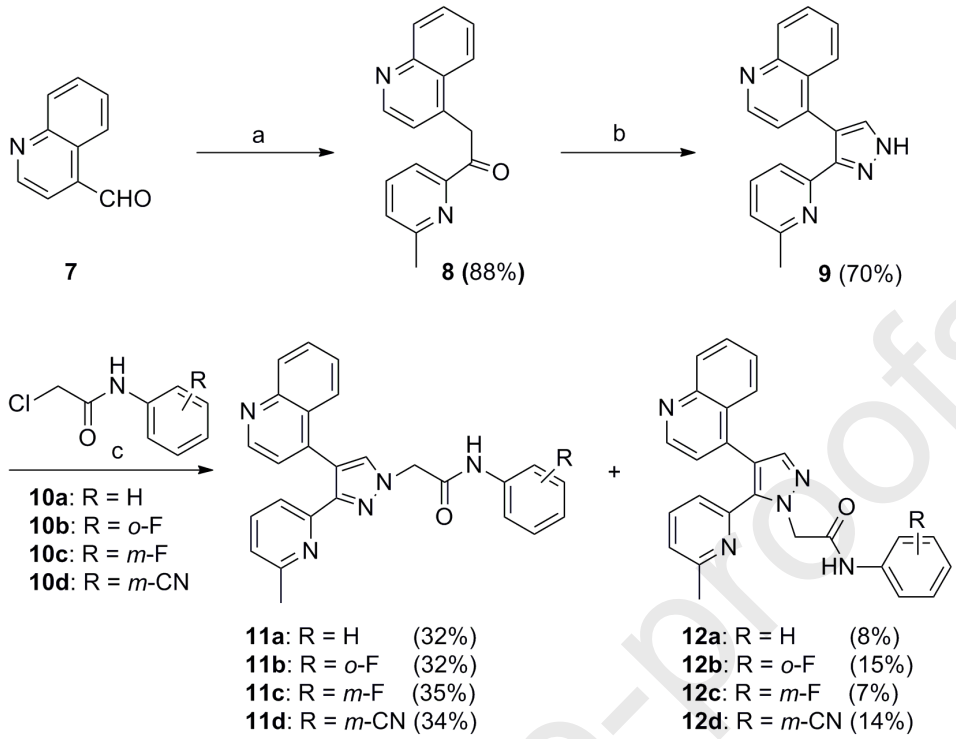

Scheme 1. Reagents and conditions: (a) (i) diphenyl(6-methylpyridin-2-yl)(phenylamino)methylphosphonate, Cs_2CO_3, THF: *i*-PrOH (4:1), rt, 16 h; (ii) 1 N HCl, rt, 1 h; (b) (i) DMF•DMA, DMF, 80°C, 4 h; (ii) N_2H_4•H_2O, EtOH, reflux, 4 h; (c) NaI (cat.), NaH, anhydrous DMF, rt, 2 h.

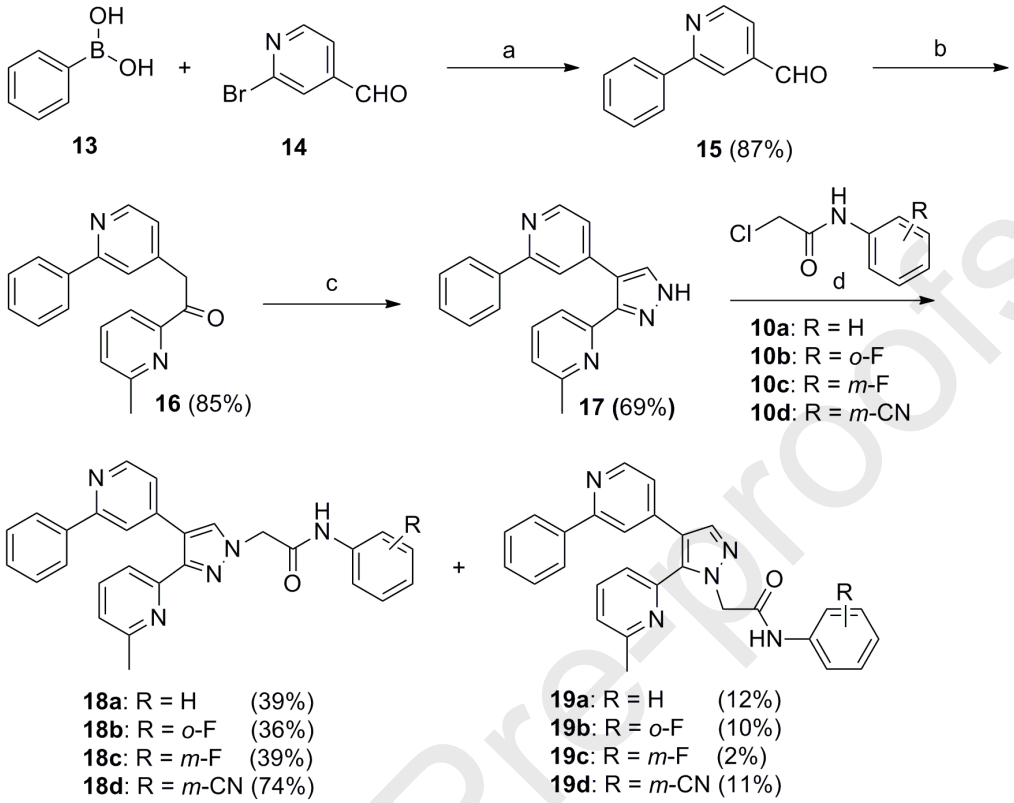

Scheme 2. Reagents and conditions: (a) Na_2CO_3, $Pd(PPh_3)_4$, THF: H_2O (10:1), reflux, 4 h; (b) (i) diphenyl(6-methylpyridin-2-yl)(phenylamino)methylphosphonate, Cs_2CO_3, THF: *i*-PrOH (4:1), rt, 4 h; (ii) 1 N HCl, rt, 1 h; (c) (i) DMF•DMA, DMF, 90°C, 4 h; (ii) $N_2H_4 \cdot H_2O$, EtOH, reflux, 4 h; (d) NaI (cat.), NaH, anhydrous DMF, rt.

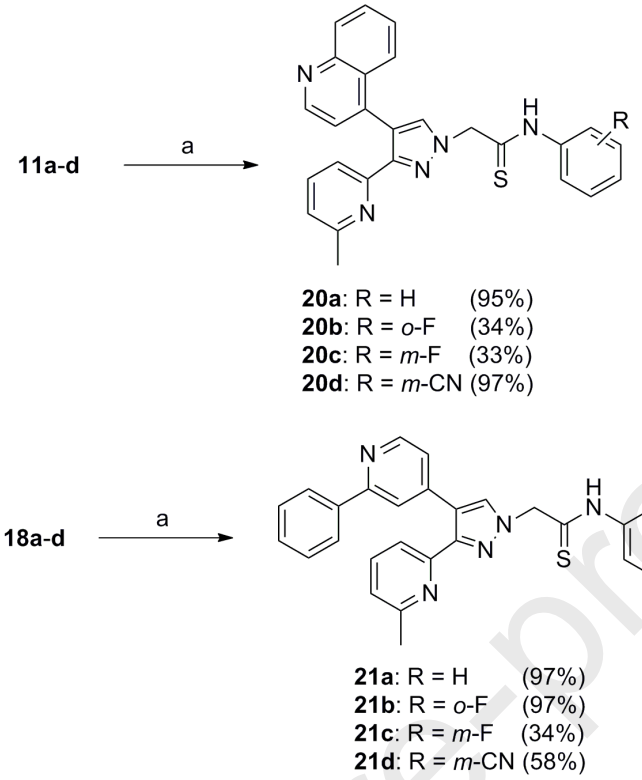

Scheme 3. Reagents and conditions: (a) Lawesson's reagent, 85°C, 4–12 h.

Table 1. Residual activities of 3(5)-(6-methylpyridin-2-yl)-4-(quinolin-4-yl)- and 3(5)-(6-methylpyridin-2-yl)-4-(2-phenylpyridin-4-yl)pyrazoles **11a–d**, **12a–d**, **18a–d**, **19a–d**, **20a–d**, and **21a–d** on ALK5 and p38α MAP kinase

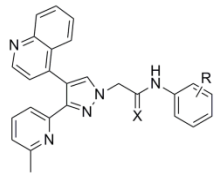

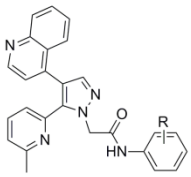

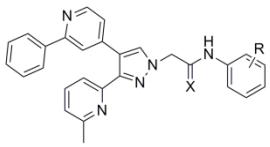

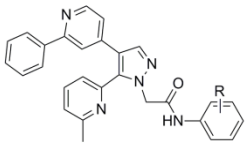

Compound	X	R	Residual activity[a,d]	
			p38α[b]	ALK5[c]
DMSO			100±0.1	100±0.1
11a	O	H	10±0	2±0
11b	O	*o*-F	6±0	0±0
11c	O	*m*-F	4±0	0±0
11d	O	*m*-CN	6±0	1±0
12a	O	H	24±0	71±1.0
12b	O	*o*-F	50±3.5	79±2.5
12c	O	*m*-F	31±0.5	39±4.0
12d	O	*m*-CN	51±3.5	17±1.0
20a	S	H	3±0.5	3±0.5
20b	S	*o*-F	4±0.5	2±0.5
20c	S	*m*-F	3±0.5	2±0.5
20d	S	*m*-CN	3±0	2±0
18a	O	H	11±1.0	12±0.5
18b	O	*o*-F	20±1.5	20±1.0
18c	O	*m*-F	14±0	3±0.5
18d	O	*m*-CN	24±0	18±0
19a	O	H	66±6.0	100±0.5
19b	O	*o*-F	96±3.5	102±2.5
19c	O	*m*-F	81±3.5	93±6.5
19d	O	*m*-CN	135±1.5	105±6.5
21a	S	H	10±1.5	11±1.0
21b	S	*o*-F	4±1.0	11±1.0
21c	S	*m*-F	9±2.5	6±0.5
21d	S	*m*-CN	15±0.5	12±0.5
4 (LY-2157299)			4±0.5	1±0

[a] Residual kinase activities were measured for each compound at 10 μM, in duplicate, in reactions containing p38α and ALK5 protein kinases. [b] p38α MAP kinase was expressed in *E. coli* as the untagged human recombinant protein. [c] ALK5 was expressed in Sf9 insect cells as the human recombinant GST-fusion protein using the vaculovirus expression system. [d] Activity is given as the mean ± SD of two independent experiments run in duplicate relative to control incubations with DMSO vehicle.

Table 2. The IC_{50} of 3(5)-(6-methylpyridin-2-yl)-4-(quinolin-4-yl)- and 3(5)-(6-methylpyridin-2-yl)-4-(2-phenylpyridin- 4-yl)pyrazoles **20a–d** and **21a–d** on ALK5 and p38α MAP kinase

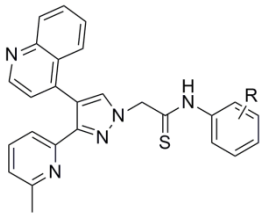

20a-d

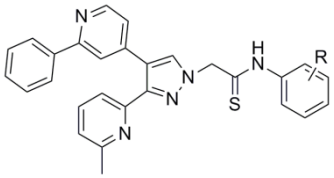

21a-d

Compound	R	IC_{50} (μM)	
		p38α[a]	ALK5[b]
20a	H	0.074±0.0002	0.057±0.0003
20b	*o*-F	0.068±0.0004	0.053±0.0004
20c	*m*-F	0.063±0.0005	0.043±0.0006
20d	*m*-CN	0.104±0.0007	0.069±0.0003
21a	H	0.536±0.0006	1.689±0.0007
21b	*o*-F	0.487±0.0008	2.050±0.0006
21c	*m*-F	0.761±0.0005	1.560±0.0004
21d	*m*-CN	1.150±0.0006	2.200±0.0003
4 (LY-2157299)		0.487±0.0005	0.119±0.0006

[a] p38α MAP kinase was expressed in *E. coli* as untagged human recombinant protein. [b] ALK5 was expressed in Sf9 insect cells as a human recombinant GST-fusion protein using the vaculovirus expression system. [a,b] Values are the average of three independent experiments run in triplicate.

Declaration of interests

☒ The authors declare that they have no known competing financial interests or personal relationships that could have appeared to influence the work reported in this paper.

☐The authors declare the following financial interests/personal relationships which may be considered as potential competing interests:

Highlights

- Six series of pyrazole derivatives were designed and synthesized.
- The effect of **J-1012** on HIF-1α activation in HCT116 cells was investigated.
- **J-1012** markedly decreased the hypoxia-induced or TNF-induced accumulation of HIF-1α protein dose-dependently.